Palaeogeography, Palaeoclimatology, Palaeoecology 595 (2022) 110979

Contents lists available at ScienceDirect

Palaeogeography, Palaeoclimatology, Palaeoecology

journal homepage: www.elsevier.com/locate/palaeo

Calibrating bulk and amino acid $\delta^{13}C$ and $\delta^{15}N$ isotope ratios between bivalve soft tissue and shell for paleoecological reconstructions

Natasha L. Vokhshoori [a,b,*], Brett J. Tipple [c,d], Laurel Teague [a], Alexander Bailess [a], Matthew D. McCarthy [a]

[a] University of California Santa Cruz, Department of Ocean Science, 1156 High Street, Santa Cruz, CA 95060, USA
[b] Smithsonian Institution National Museum of Natural History, Dept. of Anthropology, 10th St. & Constitution Ave. NW, Washington, DC 20560, USA
[c] University of California Santa Cruz, Institute of Marine Sciences, 1156 High Street, Santa Cruz, CA 95060, USA
[d] University of Utah, School of Biological Sciences, 257 S 1400 E, Salt Lake City, UT 84112, USA

ARTICLE INFO

Editor Name: Dr. Shucheng Xie

Keywords:
Bivalve shell calibration
Carbon isotopes
Nitrogen isotopes
Compound-specific isotopes of amino acids
Mytilus edulis
Ostrea lurida
Mytilus californianus

ABSTRACT

Ecological isotope proxies measured in ancient bivalve shell matrix protein have great promise for paleoecological reconstruction. Compound-specific isotopes of amino acids (CSI-AA) may be an ideal tool for developing paleoecological proxies, as initial work has indicated that CSI-AA is less subject to alteration under geologic conditions relative to bulk isotope values. While CSI-AA proxies have been applied in modern bivalve soft tissues and a few shell studies, they have yet to be systematically investigated in shell matrix protein. Here, we measured stable isotope values of carbon ($\delta^{13}C$) and nitrogen ($\delta^{15}N$) in both bulk and individual amino acids (AA), comparing soft tissue and shell organic fractions to test the fidelity of a suite of ecological isotope proxies in shell. We sampled three ubiquitous bivalve species in four seasons for one year from two common coastal environments: littoral rocky intertidal and estuarine delta ecosystems. Particulate organic matter (POM) was simultaneously collected to investigate relationships between tissue types and local POM isotope signatures. The ecological proxies tested include trophic niche breadth from bulk isotopes, and baseline $\delta^{13}C$ and $\delta^{15}N$ values, resource contribution, and trophic level from CSI-AA data. We found niche breadth corresponded well between tissue types, but that bulk isotope values were significantly higher in shell compared to soft tissue. In the CSI-AA record, there were no differences in baseline $\delta^{13}C$ and $\delta^{15}N$ proxies between tissue types. While no consistent seasonal trends were observed in the $\delta^{13}C$ record, summer bulk and baseline $\delta^{15}N$ values were lowest in both ecosystems in both tissues. Food resource contribution estimates from shell also closely matched soft tissue, however trophic level estimates were consistently higher in shell, attributed to a systematic offset in Glutamic acid $\delta^{15}N$ values. We therefore propose here a new mollusk-specific trophic discrimination factor, and corresponding shell isotope enrichment factor to correct for isotopic routing, both required for accurate paleoecological reconstructions.

1. Introduction

Bivalves and their shells are in many respects ideal bioarchives for developing detailed paleoecological records of nearshore marine primary productivity, as they feed at the base of the food chain, are abundant in coastal environments with precisely known source locations, and shell material is well preserved in both archeologic and geologic archives. Stable isotopes of carbon ($\delta^{13}C$) and nitrogen ($\delta^{15}N$) from whole tissue (bulk) and amino acids (AA) measured in the shells of bivalves therefore represent a largely unexplored source of highly detailed information into past coastal primary productivity and ecosystem trophic structure. While bulk $\delta^{13}C$ and $\delta^{15}N$ values are useful for reflecting the trophic niche of a community (Jackson et al., 2011; Newsome et al., 2007), $\delta^{13}C$ and $\delta^{15}N$ of individual AAs carry far more detailed information, recording both trophic level (Chikaraishi et al., 2009) and food resource contribution (Stock and Semmens, 2016), as well as the isotopic values at the base of its food chain (Vokhshoori et al., 2014; Shen et al., 2021), commonly referred to as the isotopic "baseline." New analytical tools and reliable paleoarchives are therefore key for understanding how natural and anthropogenic environmental

* Corresponding author at: University of California Santa Cruz, Department of Ocean Science, 1156 High Street, Santa Cruz, CA 95060, USA.
E-mail address: vokhshoorin@si.edu (N.L. Vokhshoori).

https://doi.org/10.1016/j.palaeo.2022.110979
Received 14 October 2021; Received in revised form 30 March 2022; Accepted 2 April 2022
Available online 6 April 2022

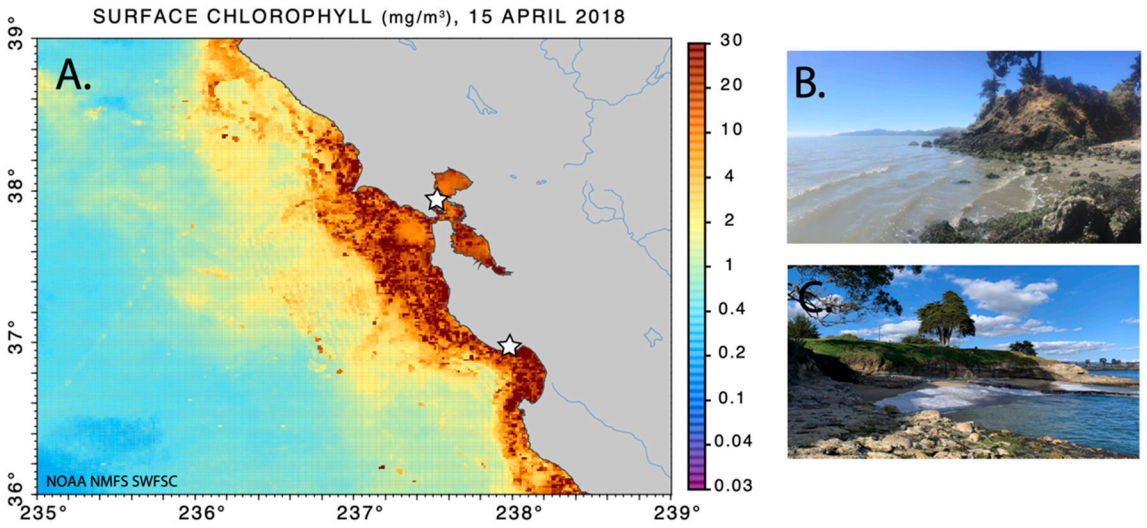

Fig. 1. Sampling locations and photographs of sampling sites. (A) Surface chlorophyll *a* (mg/m^3) for a day in the year of sampling (15 April 2018), typical production for this region, where sampling locations are denoted on map by star. Photographs of sampling sites: (B) Northern San Francisco Bay estuary (37°56′29 N, 122°28′56 W) and (C) Monterey Bay littoral upwelling system (36°57′2 N, 122°2′39 W). * SF Bay samples were from two locations indistinguishable from this map view.

changes have influenced marine ecosystems in the past, in order to understand future change and potential mitigation.

CSI-AA ecological proxies are based on the differences in fractionation of specific AAs between diet and consumer. For C, primary producers synthesize essential AAs (EAA) with a unique $\delta^{13}C$ "fingerprint" based on evolutionary divergence (Larsen et al., 2009, 2013). Since animals must acquire EAAs from their diet, $\delta^{13}C_{EAA}$ fingerprints are passed up the food chain unaltered, and thus preserve the signature of the primary producer assemblage through trophic transfers (Hare et al., 1991; Howland et al., 2003; McMahon et al., 2010). Libraries of the EAA $\delta^{13}C$ values for potential primary producer types for a given ecosystem (e.g., Larsen et al., 2009, 2013; Tipple et al., 2021) combined with Bayesian mixing models (e.g., MixSIAR; Stock and Semmens, 2016) can therefore be used for quantifying shifting baseline resource contribution to consumers within that system. For N, the "trophic AA" group (e.g., Glutamic Acid: Glu) undergo significant transamination/deamination which predictably increases the $\delta^{15}N$ values with each trophic transfer. A second group now called "Transitional AA" (e.g., Glycine: Gly and Serine: Ser) can undergo major *de novo* synthesis in a consumer (McMahon and McCarthy, 2016). Finally, a third group collectively known "source AAs" (e.g., Phenylalanine: Phe) show little to no fractionation with trophic transfer, and thus reflect baseline nitrogen values.

However, for any potential bioarchive of isotopic information, both precise trophic levels and isotope systematics must be well characterized, typically by conducting field or captive feedings studies. For example, if there are tissue-specific bulk or compound specific isotope offsets, due to isotopic routing of dietary macronutrients or other factors, calibrations will be required to reconstruct original ecosystem values. While it is generally assumed AAs from different tissue types (e.g., muscle, shell, bone, etc.) reflect common trophic enrichment patterns linked to central metabolism, specific tissues can also have characteristic isotope offsets (e.g., Wolf et al., 2015). Specifically, for paleobioarchives for example, McMahon et al. (2018) showed differences in deep-sea coral polyp tissues and its structural gorgonian proteins.

This study aims to address the fundamental methodological questions required before CSI-AA data in ancient bivalve shell can be used to reconstruct past coastal ocean changes (Ellis et al., 2014; Whitney et al., 2019). We present the first paired $\delta^{13}C$ and $\delta^{15}N$ data in bulk and individual AAs in both shell matrix protein and soft tissue of three marine bivalves species. Bivalves were collected live from two well-characterized coastal environments – Monterey Bay littoral upwelling system and northern San Francisco Bay estuarine-delta system, seasonally over one year. Olympia oysters (*O. lurida*), and blue mussels (*M. edulis*) were collected from the estuarine site and California mussels (*M. californianus*) from the littoral upwelling site, along with seawater particulate organic matter (POM) to directly assess the impacts of seasonal food source dynamics at the base of the food web on CSI-AA and bulk isotopic signals recorded in contrasted tissues of these bivalve species. For our primary goal of exploring CSI-AA ecological proxies, we address two main questions: 1.) can combined bulk and AA isotope techniques be used in bivalve shells to reconstruct detailed records of coastal primary productivity, and 2.), if yes, what calibrations are required?

2. Materials & methods

2.1. Study location and site description

Sampling occurred at two ubiquitous, well-characterized coastal environments along California's coast: Littoral rocky intertidal zone of Monterey Bay (36°57′2 N, 122°2′39 W) and San Francisco Bay estuary (37°56′29 N, 122°28′56 W, spring sampling site: 37°39′50 N, 122°23′21 W) (Fig. 1). The Monterey Bay is characterized by strong seasonal upwelling that occurs in spring and early summer which supplies cold, nutrient rich waters to the surface stimulating high primary production, predominantly composed of diatoms and dinoflagellates. Interannual and decadal oceanic variability due to ENSO and PDO can strongly affect average sea surface temperature (SST) and upwelling intensity on the coast, where the strongest El Niño events (i.e., above average SST and weakened upwelling) coincide with positive phases of the PDO (Jacox et al., 2015).

Northern San Francisco (SF) Bay is characterized as a partially mixed estuary (Cloern, 1996), where nutrients are supplied from both marine inflow through a narrow deep channel (via the Golden Gate) and freshwater runoff from the Sacramento-San Joaquin River Delta system (Jassby et al., 1993). The confluence of marine and freshwater sources produces spatial gradients of salinity, suspended sediments, nutrients and biological communities (Cloern, 1996). This dynamic estuary is regulated by seasonal winter storm events and also diurnal tidal currents through the Golden Gate channel, both mechanisms contributing different organic carbon sources. Together, these hydrodynamics supply a mixture of marine and terrestrial primary producers, including various phytoplankton species (marine and freshwater), vascular plants (woody terrestrial and submerged), seagrasses and macroalgae (Cloern et al., 2002).

2.2. Sample collection and processing

Whole individuals 55–60 mm of California mussel (*M. californianus*), Olympia oyster (*O. lurida*) and Blue mussel (*M. edulis*), as well as seawater particulate organic matter (POM) collected seasonally between February 2018 to January 2019: Spring (Apr./May), Summer (Jun./Jul.), Fall (Oct.) and Winter (Jan.), with *M. californianus* collected at the littoral site, and *O. lurida* and *M. edulis* at the estuarine site. 3–10 whole individual bivalves were collected in each season, with more frequent sampling at the littoral site; simultaneously 5–10 L of seawater were collected in acid-washed 5-L Nalgene bottles and remained chilled in a cooler until POM filtration in the lab.

Seawater was pre-filtered through a Nitex mesh (53 μm) then filtered onto combusted 47 mm 0.7 μm GF/F filters. Typically, 3 L and 300 mL of littoral seawater and estuarine water was filtered onto a single filter, respectively. Sample yields were calculated using pre-weighed filters, a wedge of which was removed for bulk isotope analysis, and the remaining filtrate and filter transferred to hydrolysis vials for CSI-AA.

Bivalves were dissected for the muscle adductor tissue, rinsed with deionized water, stored frozen, then lyophilized for 24 to 48 h; the remaining soft tissue parts were discarded. Mussel soft tissue was then homogenized and ~ 0.5 mg was weighed into tin capsules for bulk isotope analysis. Bivalve shells were scrubbed clean using a wire brush and scalpel, then soaked in a dilute bath of bleach (NaOCl) for 1 h at room temperature, sonicated in nano-pure water, and dried overnight at 60 °C. Each shell was then crushed using a mortar and pestle, and sieved through a 5 μm screen. For bulk $\delta^{15}N$ analysis, ~35 mg of non-acidified (i.e., non-demineralized) crushed whole shell was weighed into tin capsules and another 1000 mg was weighed into a labelled 20x150mm borosilicate vial for shell demineralization. To extract the organic matter (OM) fraction, samples were acidified with 1 N HCl by pipetting 1 mL increments until shell was completely dissolved (~35 mL); samples were stored 4 °C overnight to complete the reaction. After acidification, OM fraction was isolated by filtration onto pre-weighed 22 mm 0.7 GF/F filters, rinsed to neutrality with nano-pure water, and dried overnight at 60 °C. Sample yields were calculated, ~0.5 mg was weighed into tin capsules for bulk $\delta^{13}C$ analysis, and the remaining amount was used for CSI-AA.

2.3. Bulk stable isotope analysis

Stable isotopes of carbon ($\delta^{13}C_{bulk}$) and nitrogen ($\delta^{15}N_{bulk}$) were measured by the University of California Santa Cruz Stable Isotope Laboratory (UCSC-SIL) using a CE Instruments NC2500 elemental analyzer coupled to a Thermo Scientific DELTAplus XP isotope ratio mass spectrometer via a Thermo-Scientific Conflo III. For high C content samples, automated in line CO_2 trapping is used to remove interference with N_2. Isotopes values are reported using delta (δ) notation: $\delta^{13}C$ or $\delta^{15}N = [(R_{sample}/R_{standard}) - 1] \times 1000$, where R is the ratio of rare to common isotope of the sample (R_{sample}) and standard ($R_{standard}$), respectively, and corrected to VPDB (Vienna PeeDee Belemnite) for $\delta^{13}C$ and AIR for $\delta^{15}N$ against an in-house gelatin standard reference material (PUGel; ($\delta^{13}C = -12.6‰$, $\delta^{15}N = 5.6‰$) which is extensively calibrated against international standard reference materials. Measurements are corrected for size effects, blank-mixing effects, and drift effects. An externally-calibrated Acetanilide standard reference material ($\delta^{13}C = -29.5‰$, $\delta^{15}N = 1.1‰$) purchased from Dr. Arndt Schimmelmann of Indiana University is measured as a sample for independent quality control. Typical isotope ratio precision (1σ) is <0.1‰ VPDB for $\delta^{13}C$ and < 0.2‰ AIR for $\delta^{15}N$.

2.4. Amino acid stable isotope analysis

The stable carbon ($\delta^{13}C_{AA}$) and nitrogen ($\delta^{15}N_{AA}$) isotope values of amino acids from composites of bivalve soft tissue and demineralized shell OM, and seawater POM were analyzed following Batista et al., 2014. Briefly, ~5 mg dry weight bivalve shell protein and soft tissue, and ~ 5–8 mg seawater POM sample on GF/F filters were weighed into 8 mL hydrolysis vials, submerged in 1–2 mL of 6 N HCl, purged with N_2 gas to remove oxygen, and hydrolyzed for 20 h at 110 °C. After hydrolysis, samples were cooled to room temperature and stored in a −4 °C freezer until further processing. Samples were then purified using cation-exchange chromatography with the DOWEX 50WX8–400 resin. Before dry down, purified filtrate was spiked with Norleucine as an internal standard.

$\delta^{15}N$-AA and $\delta^{13}C$-AA values were measured as trifluoroacetyl isopropyl ester (TFA-IP) derivatives. After drying hydrolysates at 60 °C under N_2, amino acid isopropyl esters were prepared with a 1:4 mixture of acetyl chloride:isopropanol at 110 °C for 60 min and then aceytlated using a 1:1 mixture of dichloromethane (DCM) and trifluoroacetic anhydride (TFAA) at 110 °C for 10 min (Silfer et al., 1991). Samples were again dried and finally re-dissolved in ethyl acetate for GC-IRMS analysis. AA isotopes values were measured using a Thermo Trace gas chromatograph coupled to a Finnegan Delta-Plus IRMS and GCC III (isoLink) at the UCSC-SIL. Using this method, we measured $\delta^{15}N$ and $\delta^{13}C$ values of the following AAs: alanine (Ala), glycine (Gly), threonine (Thr), serine (Ser), valine (Val), leucine (Leu), isoleucine (Ile), proline (Pro), aspartic acid (Asp), glutamic acid (Glu), phenylalanine (Phe), tyrosine (Tyr), and lysine (Lys). All sample derivatives were injected/quantified in triplicate. Measured $\delta^{13}C_{AA}$ values were corrected for the carbon atoms added during derivatization following the approach of Silfer et al. (1991) and Hare et al. (1991). Final isotope value accuracy and reproducibility was checked in two ways: first by comparison of the internal Norleucine standard with its known values, and second by assessing values of an in-house long-term McCarthy lab reference material (cyanobacteria), analyzed with every sample set according to McCarthy Lab protocols (Batista et al., 2014). Reproducibility, as estimated with standard deviation for samples, was on average less than <0.3‰ (range: 0.0–0.6‰) for carbon and < 0.5‰ (range: 0.1–1.3‰) for nitrogen.

2.5. Amino-acid ecological parameter definitions and statistics

We calculate CSI-AA trophic level using the most common formulation (algae data-based) from Chikaraishi et al. (2009),

$$TL_{CSIA} = 1 + \left[\delta^{15}N_{Glu} - \delta^{15}N_{Phe} - \beta / TDF_{Glu-Phe}\right], \quad (1)$$

where $\delta^{15}N_{Glu}$ and $\delta^{15}N_{Phe}$ represent the stable nitrogen isotope values of bivalve Glu and Phe, respectively, β is a constant which represents the assumed difference in $\delta^{15}N$ between Glu and Phe of primary producers (3.4‰ for aquatic cyanobacteria and algae; McClelland and Montoya, 2002; Chikaraishi et al., 2009), $TDF_{Glu-Phe}$ is defined as $\Delta^{15}N_{Glu} - \Delta^{15}N_{Phe}$, but reflects an assumed average change in $\delta^{15}N$ of Glu and of Phe of 7.6‰ (Chikaraishi et al., 2009), while our newly proposed mollusk-specific $TDF_{Glu-Phe}$ is 3.4‰ ($TL_{CSIA-mollusk}$; this study) based on our measured data corresponding to a single trophic transfer for filter-feeding mollusks (see section 3.5). Finally, ε_{shell} (see section 3.5) is the new term proposed for the mollusk specific equation, representing the observed additional average fractionation in Glu (1.6‰) between tissue and shell, presumably due to isotopic routing to the shell protein biomineral fraction.

Baseline isotope values were estimated from common CSI-AA parameters. For $\delta^{15}N_{baseline}$ based on past work in mollusks (Vokhshoori and McCarthy, 2014) we used the non-fractionating source AA Phenylalanine.

$$\delta^{15}N_{Baseline} = \delta^{15}N_{Phe}, \quad (2)$$

where $\delta^{15}N_{Phe}$ is the isotope value of Phenylalanine in a mollusk or seawater particulate organic matter.

For $\delta^{13}C_{baseline}$ we used the equation from Shen et al. (2021) for exported production in the nearshore California Current:

$$\delta^{13}C_{Baseline} = 0.75 \times \delta^{13}C_{EAA} - 5.9 \quad (3)$$

where $\delta^{13}C_{EAA}$ is the mol% adjusted measured average $\delta^{13}C$ of all EAAs (Ile, Leu, Lys, Phe, Thr and Val), 0.75 is the slope of a line between measured $\delta^{13}C_{bulk}$ and $\delta^{13}C_{EAA}$ values of suspended POM from the Monterey Bay and 5.9 is the associated y-intercept (Shen et al., 2021).

For statistical analyses, *t*-tests, ANOVAs and mixing models were performed in R (v.3.3.1) with RStudio interface (v.0.98.1028). Normality (Q-Q plots) and homoscedasticity (Bartlett's test) of the data were verified before statistical analyses. From bulk isotopes, we calculated total area (TA) and standard ellipse areas (SEA; $n > 10$) for each site population using the stable isotope Bayesian ellipses in R package (SIBER; Jackson et al., 2011), and with normalized EAA $\delta^{13}C$ values we used the Bayesian mixing model stable isotope analysis in R package (MixSIAR; Stock and Semmens, 2016) to estimate resource contribution to bivalve diet using a "training set" of potential endmember sources from Larsen et al., 2009, 2013 and Tipple et al., 2021.

3. Results

3.1. Bulk isotope values and niche widths between species –

M. californianus muscle tissue $\delta^{13}C$ values (−15.6 ± 0.3‰, $n = 54$) were significantly different from estuarine species; *M. edulis* (−22.0 ± 0.9‰, $n = 15$) and from *O. lurida* (−23.2 ± 0.6‰, $n = 37$) tissues (Tukey HSD *t*-test $P < 0.001$) (Table 1). Similarly, *M. californianus* muscle tissue $\delta^{15}N$ values (11.0 ± 0.4‰) were significantly different from estuarine species (*M. edulis*, 12.3 ± 1.0‰ and also from *O. lurida*, 12.7 ± 1.1‰) ($P < 0.001$). $\delta^{15}N$ values of the two estuarine species were not significantly different ($P = 0.14$), while *O. lurida* $\delta^{13}C$ values were ~ 1‰ lower than *M. edulis* ($P < 0.0001$).

Isotope values of bulk shell matrix protein displayed similar patterns to those of the muscle tissues. *M. californianus* tissue $\delta^{13}C$ values (−14.5 ± 0.3‰, $n = 22$) were higher and significantly different from both *M. edulis* (−20.0 ± 0.8‰, n = 15) and *O. lurida* (−21.3 ± 1.6‰, n = 15) (Tukey HSD t-test $P < 0.001$) (Table 1). Similarly, *M. californianus* shell $\delta^{15}N$ values (12.1 ± 0.3‰) were lower and significantly different from both estuarine species (*M. edulis*, 12.9 ± 0.9‰ and *O. lurida*, 13.4 ± 1.1‰) ($P < 0.001$). $\delta^{15}N$ values of the two estuarine species were not significantly different ($P = 0.19$), while *O. lurida* $\delta^{13}C$ values were again ~ 1‰ lower than *M. edulis* ($P = 0.004$).

Comparing shell to tissue, average shell stable isotope values were always more enriched in the heavy isotope (both $\delta^{13}C$ and $\delta^{15}N$) (Table 2). These isotopic offsets were significantly different in all cases (Tukey HSD *t*-test, $P < 0.01$). The average $\delta^{13}C$ offset in shell from tissue was 1.2‰ and 2‰ in the littoral and estuarine ecosystem, respectively. The $\delta^{15}N$ shell and tissue offsets were on average 1‰ higher in shell OM for all species.

Standard ellipse areas (SEA) represent the isotopic niche width (units: ‰^{2}) as reflected by bulk muscle or shell matrix protein $\delta^{13}C$ and $\delta^{15}N$ biplots for the three species of bivalves (Fig. 2, Fig. S1), and is informative for understanding community composition and structure (i.e., generalists vs. specialists). Among species, soft tissue *M. californianus* had the smallest niche width (0.32‰^{2}; $n = 54$) and total area (TA = 1.49‰^{2}). While soft tissue SEA of *M. edulis* (2.40‰^{2}; $n = 18$) was larger than in *O. Lurida* (1.79‰^{2}; $n = 46$), the total area (TA) of isotope values for *O. Lurida* was larger (7.44‰^{2}) than *M. edulis* (5.03‰^{2}). Shell matrix protein SEA results were very similar to soft tissue SEA, where *M. californianus* was 0.32‰^{2} ($n = 22$), *M. edulis* was 1.48‰^{2} ($n = 15$) and *O. Lurida* was 2.22‰^{2} ($n = 15$).

3.2. Bulk isotope values in particulate organic matter and offsets from bivalve tissue

Table 3 reports seawater particulate organic matter (POM) Nitex (>53 μm) and GFF (<0.7 μm) sample sizes, mean isotope values (±SD) and ranges (Table S1 additionally breaks out specific values by season). For both isotopes in both ecosystems, Nitex and GFF POM values were not statistically different (Tukey HSD t-test, $P > 0.05$), therefore data for both size fractions were combined, and reported as POM averages for each sampling period. At the littoral site, average seasonal $\delta^{13}C$ values of combined POM was −18.6 ± 1.7‰, ranging from −23.2 to −15.3‰; the corresponding average seasonal $\delta^{15}N$ value was 9.1 ± 2.2‰, however with a far greater range, from 3.9 to 14.1‰. At the estuarine site, the average $\delta^{13}C$ value of combined POM was −22.4 ± 1.4‰, ranging from −23.7 to −19.7‰, and for $\delta^{15}N$ the average value was 9.9 ± 1.6‰,

Table 2
Mean bulk $\delta^{13}C$ and $\delta^{15}N$ offset (‰) between muscle tissue and shell organic matter in three bivalve species. Asterisk denotes degree of significant difference ($P > 0.05$, *$P < 0.05$, **$P < 0.01$, ***$P < 0.001$).

	n	Mean Offset	SD	Min	Max	Range
$\delta^{13}C$ (‰)						
Littoral Mussel	28	1.2***	0.4	0.2	1.8	1.6
Estuarine Mussel	18	2.1***	0.4	1.4	3.0	1.6
Estuarine Oyster	17	1.9***	1.2	0.9	3.3	4.3
$\delta^{15}N$ (‰)						
Littoral Mussel	22	1.0***	0.4	0.0	1.7	1.6
Estuarine Mussel	18	0.9*	0.7	0.0	2.4	2.4
Estuarine Oyster	19	0.8**	0.8	0.5	3.1	3.5

Table 1
Mean bulk $\delta^{13}C$ and $\delta^{15}N$ values (‰) and standard deviation from muscle and shell organic matter by season and each bivalve species overall mean for *Mytilus californianus*, estuarine *O. Lurida* and *M. edulis*. Different superscript letters denote significant difference (ANOVA, $P < 0.05$).

Season	$\delta^{13}C_{muscle}$	SD	$\delta^{13}C_{Shell}$	SD	$\delta^{15}N_{muscle}$	SD	$\delta^{15}N_{Shell}$	SD
Littoral Mussel (*M. californianus*)								
Spring	-15.6^{a}	0.3	-14.5^{a}	0.3	11.1^{a}	0.4	12.2^{a}	0.2
Summer	-15.5^{a}	0.2	-14.8^{ab}	0.3	10.6^{b}	0.3	11.8^{a}	0.5
Fall	-15.5^{a}	0.2	-14.2^{ac}	0.1	11.1^{a}	0.4	12.0^{a}	0.2
Winter	-15.7^{a}	0.2	-14.5^{a}	0.3	11.1^{a}	0.3	12.2^{a}	0.3
Overall mean	−15.6	0.3	−14.5	0.3	11.0	0.4	12.1	0.3
Estuarine Oyster (*Ostrea lurida*)								
Spring	-23.6^{a}	0.5	-23.5^{a}	0.3	12.7^{a}	0.6	13.7^{ab}*	0.5
Summer	-23.5^{a}	0.6	-21.2^{b}	0.4	11.1^{b}	0.3	12.2^{a}	1.1
Fall	-23.0^{a}	0.5	-20.4^{b}	0.8	13.3^{a}	0.6	14.0^{b}	0.6
Winter	-23.1^{a}	0.3	-20.5^{b}	0.5	13.0^{a}	0.7	14.2^{b}	0.2
Overall mean	−23.3	0.5	−21.3	1.4	12.5	1.1	13.4	1.1
Estuarine Mussel (*Mytilus edulis*)								
Spring	-20.2^{a}	0.0	-18.4^{a}	0.5	12.0^{a}	0.1	14.2^{ab}	0.5
Summer	-22.8^{bd}	0.2	-20.3^{b}	0.4	11.3^{ab}	0.4	12.2^{ac}	0.5
Fall	-22.7^{b}	0.5	-20.5^{b}	0.4	11.9^{a}	0.6	12.6^{a}	0.3
Winter	-22.0^{bc}	0.3	-19.9^{b}	0.5	13.1^{ac}	1.0	13.4^{a}	1.0
Overall mean	−22.2	0.9	−20.0	0.8	12.1	0.9	12.9	0.9

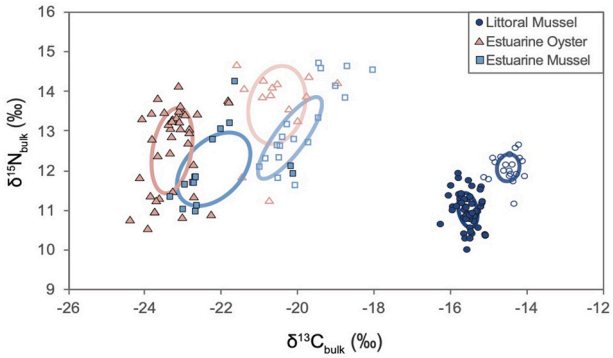

Fig. 2. Biplot of bivalve muscle tissue (filled symbols) and shell matrix protein (open symbols) bulk $\delta^{13}C$ and $\delta^{15}N$ values organized by species, littoral *Mytilus californianus* (dark blue circle, $n = 54$), estuarine *O. Lurida* (pink triangle, $n = 37$) and estuarine *M. edulis* (light blue square, $n = 15$). The colored ellipses represent the standard ellipse areas (SEA) for each of the groups. (For interpretation of the references to colour in this figure legend, the reader is referred to the web version of this article.)

Table 3
Seasonal to monthly ranges and average bulk $\delta^{13}C$ and $\delta^{15}N$ values (±1 SD) in two size fractions of seawater particulate organic matter: Nitex (>53 μm) and GFF (0.7 μm) from two coastal environments, Littoral (Santa Cruz, CA) and Estuary (Northern San Francisco Bay).

	n	Mean	SD	Max	Min	Range
Littoral POM						
$\delta^{13}C$ (‰)						
GFF	9	−19.0	0.7	−18.1	−20.1	2.0
Nitex	10	−18.3	2.2	−15.3	−23.2	8.0
Combined	19	−18.6	1.7	−15.3	−23.2	8.0
$\delta^{15}N$ (‰)						
GFF	10	8.8	2.9	14.1	3.9	10.3
Nitex	10	9.4	1.4	13.1	7.6	5.5
Combined	20	9.1	2.2	14.1	3.9	10.3
Estuarine POM						
$\delta^{13}C$ (‰)						
GFF	5	−21.8	1.4	−20.0	−23.7	3.7
Nitex	6	−22.0	1.5	−19.7	−23.7	4.0
Combined	11	−21.9	1.4	−19.7	−23.7	4.0
$\delta^{15}N$ (‰)						
GFF	4	9.2	1.4	10.7	7.7	2.9
Nitex	6	10.4	1.3	12.7	9.4	3.3
Combined	10	9.9	1.4	12.7	7.7	5.0

ranging from 7.7 to 12.7‰.

Bulk isotopic offsets between bivalve tissue and seawater POM were different at the estuarine vs. littoral sites (Table S2). At the littoral site, *M. californianus* $\delta^{13}C_{bulk}$ values in soft tissue were 3.4 ± 0.3‰ greater than POM, and $\delta^{15}N$ values were 2.0 ± 1.4‰ greater. The shell matrix offsets were about 1‰ higher in both isotopes. At the estuarine site, offsets were more variable. Soft tissue *O. Lurida* $\delta^{13}C$ values were 1.1 ± 1.2‰ *less* than POM, while *M. edulis* $\delta^{13}C$ values were 0.3 ± 1.4‰ greater. For $\delta^{15}N$ values, *O. Lurida* was 3.4 ± 1.8‰ greater than POM and *M. edulis* was 3.0 ± 1.1‰ greater. Shell matrix protein $\delta^{13}C$ offsets were ~ 2‰ higher than muscle tissue for both bivalve species, while $\delta^{15}N$ offsets were 1‰ greater in shell than muscle tissue.

3.3. Seasonal differences in bulk isotope records

Seasonal $\delta^{13}C$ and $\delta^{15}N$ dynamics observed in the muscle soft tissue were generally also reflected in the shell matrix protein (Fig. 3, Table 1), even though the integration times are very different for these tissues: muscle tissue turnover rates are on the order of months (Gorokhova and Hansson, 1999) while shell is over the lifetime of the individual (in this study ~1 to 2 years). Littoral summer (Jul.) $\delta^{15}N$ values were significantly lower in the muscle tissue (ANOVA, $F_{3,50} = 1.89$, $P < 0.05$), and also lowest observed in the shell protein, although not significant ($F_{3,25} = 3.565$, $P > 0.03$). In contrast, *M. californianus* $\delta^{13}C$ values in muscle were not significantly different between seasons ($F_{3,50} = 1.89$, $P > 0.05$), except between summer and fall ($F_{3,25} = 3.565$, $P < 0.03$).

The estuarine environment also displayed low summer (Jun.) $\delta^{15}N$ values in both species. *O. Lurida* $\delta^{15}N$ values were significantly lower for summer in both muscle tissue ($F_{3,35} = 31.46$, $P < 0.0001$) and in shell ($F_{3,14} = 7.97$, $P < 0.01$). In *M. edulis* summer $\delta^{15}N$ values were also lowest, but not significantly different, in both muscle ($F_{3,14} = 1.53$, $P = 0.25$) and shell ($F_{3,14} = 1.59$, $P = 0.24$).

For $\delta^{13}C$, similar to the littoral ecosystem, estuarine *O. Lurida* $\delta^{13}C$ values in muscle were not statistically different between seasons ($F_{3,19} = 2.935$, $P > 0.05$). Shell $\delta^{13}C$ values also generally showed no statistical differences, with the exception that spring $\delta^{13}C$ in shell was significantly more negative than the other seasons ($F_{3,10} = 20.34$, $P < 0.0001$). It should be noted however, that as discussed in the methods section, the estuarine site sampled for the spring season was at a slightly different location in Northern SF Bay, and this might contribute to some of the differences observed in Spring. For the *M. edulis*, muscle tissue $\delta^{13}C$ values were significantly different between seasons ($F_{3,11} = 41.71$, $P < 0.0001$), and in shell Spring was significantly different from the rest of the seasons ($F_{3,11} = 10.47$, $P < 0.001$) but also the sample size was much smaller ($n = 3$ to 5 per season versus 5 to 10) and could explain the higher variability in this group.

3.4. Amino acid molar abundance

Amino acid relative molar distributions ($Mol\%_{AA}$) displayed major differences between tissue types (Fig. 4, Fig. S2), however as would be expected $Mol\%_{AA}$ was similar within each tissue type. Soft muscle tissue overall $Mol\%_{AA}$ was not significantly different between species: Glutamic acid was the most abundant (20%) followed by Leucine (15%) then Alanine and Aspartic acid (10%), with relatively minor (<5%) contributions by other AAs. However, there were nevertheless some significant differences in muscle tissue between *O. Lurida* and the two mussel species, *M. californianus* and *M. edulis*; most notably oyster Mol% Gly was lower ($F_{2,9} = 12.51$, $P < 0.01$), Leu was higher ($F_{2,9} = 17.32$, $P < 0.001$), and Ser was also higher ($F_{2,9} = 32.17$, $P < 0.0001$). By contrast $Mol\%_{AA}$ distributions in shell protein were distinct from muscle tissue across all species. Glycine and Alanine were the most abundant (20–30 Mol%), followed by Serine (12–13%) and Aspartic Acid (8.5–10%), with again only small contributions by all other AA. Again, *O. Lurida* shell $Mol\%_{AA}$ was significantly different from the two mussel species where Gly was much higher ($F_{2,9} = 16.77$, $P < 0.001$), Leu was lower ($F_{2,9} = 61.39$, $P < 0.0001$), and Pro was higher ($F_{2,9} = 192.4$, $P < 0.0001$).

3.5. Amino acid carbon and nitrogen isotope values, patterns, and tissue offsets

Measured amino acid $\delta^{13}C$ showed a remarkably similar patterns between species in both muscle tissue and shell protein. Across all three species, $\delta^{13}C_{EAA}$ patterns were very similar between shell and muscle tissue, with differences typically in the range of analytical error (<1‰; Fig. 5a). We note that littoral spring season data was not included in offset calculations because of the apparently anomalous values measured in the soft tissue for that season only (Fig. S3). The average $\delta^{13}C_{EAA}$ offset (shell – muscle tissue) was small and typically within the range of analytical variation for this analysis (see methods): 0.4‰ in *M. californianus*, −0.6‰ in *O. Lurida* and − 0.3‰ in *M. edulis*. In contrast to the essential amino acids, the offsets in the $\delta^{13}C_{NEAA}$ were larger and also showed much more variability, particularly in *M californianus* (Fig. 5).

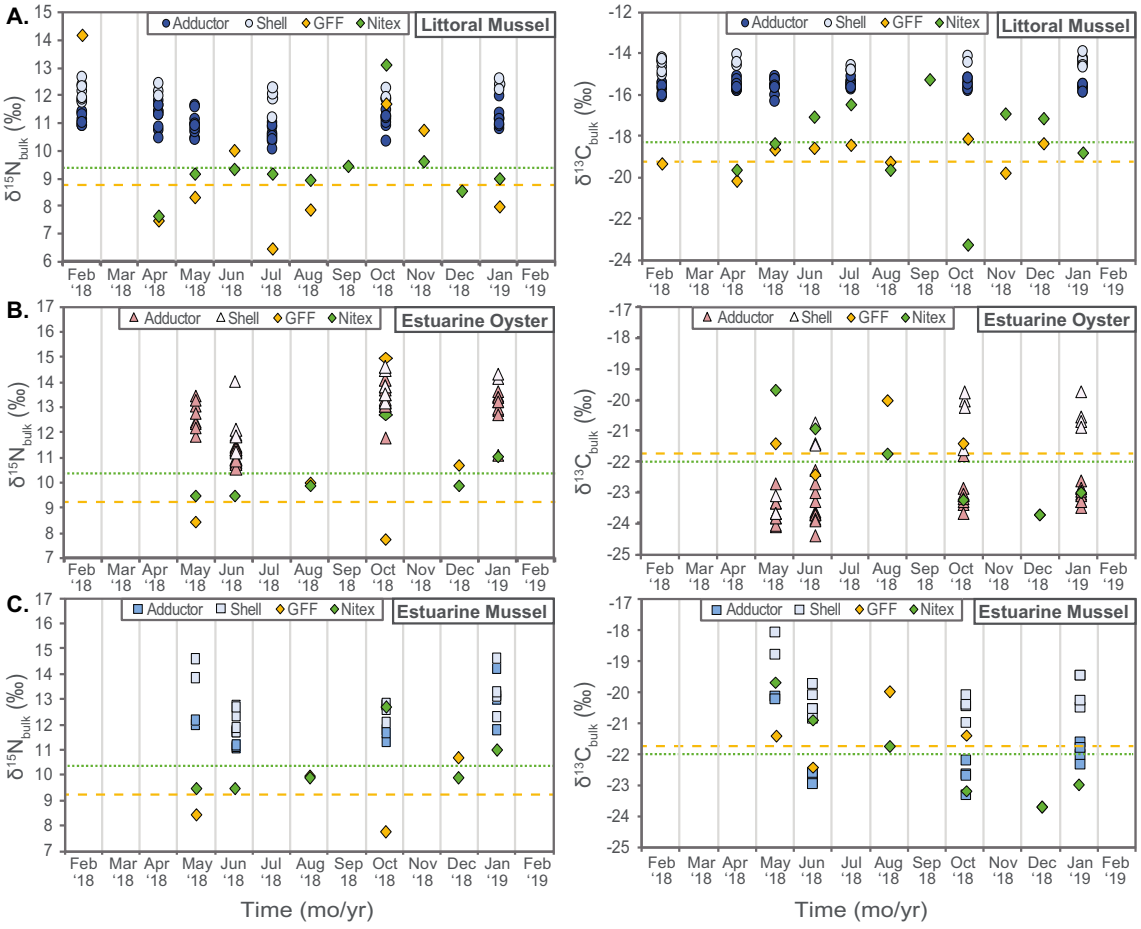

Fig. 3. Bulk $\delta^{13}C$ and $\delta^{15}N$ values of bivalve and seawater particulate organic matter organized by month of sampling. Bivalve muscle adductor tissue (dark shading) and shell matrix protein (light shading) for three bivalve species in this study: (A) littoral *Mytilus californianus*, (B) estuarine *O. Lurida* and (C) estuarine *M. edulis*. Plotted with bivalve tissue isotope values are two size fractions of seawater POM: GFF (>0.7 μm, yellow diamond) and Nitex (>53 μm, green diamond). Mean of the two POM size fractions are shown for reference indicated by the colored dotted and hashed line (GFF, yellow dashed; Nitex, green dotted). (For interpretation of the references to colour in this figure legend, the reader is referred to the web version of this article.)

The measured amino acid $\delta^{15}N$ value comparisons between species and tissue types showed the expected overall CSI-AA pattern, with Trophic AAs consistently more enriched than the Transitional (e.g., Gly, Ser) and Source AAs (e.g., Phe, Lys) (Fig. S4). However, there were also a few notable differences. In *O. Lurida* $\delta^{15}N_{Ile}$ and $\delta^{15}N_{Leu}$ values were consistently lower, by ~4‰, relative to all other Trophic AAs in both tissue types, an offset not observed in two mussel species.

Between tissue types, consistent offsets were observed in the trophic and transitional AA groups, but not the Source AAs. For specific AA groupings, the average $\delta^{15}N_{Tr\text{-}AA}$ offset was similar between species: 1.8‰ in *M. californianus*, 1.5‰ in *O. Lurida* and 1.1‰ in *M. edulis*. Specifically, $\delta^{15}N_{Glu}$ (the canonical trophic-AA used in the TL_{CSIA} equation), the average offset among all species was 1.9 ± 1.6‰ (range − 0.4 to 4.1‰). The two transitional AAs, Gly and Ser behaved differently between the bivalve genus; *O. Lurida* $\delta^{15}N$ offsets were 3‰ in shell, but 2‰ lower in *M. californianus* and *M. edulis*. Conversely, the average offset between tissue types in $\delta^{15}N_{Phe}$, the canonical source-AA used in the TL_{CSIA} equation and the proxy for $\delta^{15}N_{Baseline}$ value, was within the range of analytical error (0.4 ± 0.9‰; range − 0.9 to 1.5‰). Lys, the other Source AA, also showed minimal offset, −0.3 ± 1.2‰; range − 1.7 to 1.4‰. For Thr, which is often considered an 'inverse" trophic AA (that is, displaying $\delta^{15}N$ depletion with trophic transfer; e.g., McMahon and McCarthy, 2016, Mompean et al., 2016) negative offsets between tissue and shell were consistently observed.

3.6. CSI-AA ecological proxies

Four CSI-AA ecological proxies were calculated and compared between tissue types: $\delta^{13}C_{baseline}$, $\delta^{15}N_{baseline}$ (Fig. 6), food resource contribution from Bayesian modeling output (Fig. 7), and trophic level (Fig. 8). Average $\delta^{13}C_{baseline}$ was essentially identical (less than 1‰ difference) between tissue types in all species. $\delta^{13}C_{baseline}$ values in muscle tissue and shell matrix protein in *M. californianus* was −19.1 ± 1.5‰ versus −20.7 ± 0.4‰, respectively; *M. edulis* was −24.8 ± 0.9‰ versus −25.7 ± 2.1‰, respectively; and *O. lurida* was −25.8 ± 1.1‰ versus −25.7 ± 1.6‰, respectively. Similarly, $\delta^{15}N_{baseline}$ (defined here as the source AA $\delta^{15}N_{Phe}$; see methods) also showed little to no offset between muscle tissue and shell matrix protein across all species: *M. californianus* was 8.8 ± 0.7‰ versus 9.2 ± 0.3‰, respectively; *M. edulis* was 9.5 ± 0.6‰ versus 10.3 ± 1.4‰, respectively; and *O. lurida* was 11.0 ± 1.1‰ versus 10.6 ± 0.9‰, respectively.

Resource contribution based on $\delta^{13}C_{EAA}$ using the Bayesian mixing model MixSIAR (Fig. 7) were also very similar between shell and muscle tissue in all bivalves. Model output indicated that the *M. californianus* diet was ~80% microalgae in both tissues followed by smaller amounts of microalgae (10–15%) and bacteria (10–15%). Model estimates indicated similar relative resource proportions in *M. edulis* and *O. lurida* with 55–60% of algae (micro- and macro- combined), followed by ~20% bacteria and ~ 20–25% plants (terrestrial and aquatic combined).

In contrast, Trophic level (TL) estimations (Fig. 8) using Eq. 1 were substantially lower than expected for bivalves, ranging from 1.3 to 1.5 in

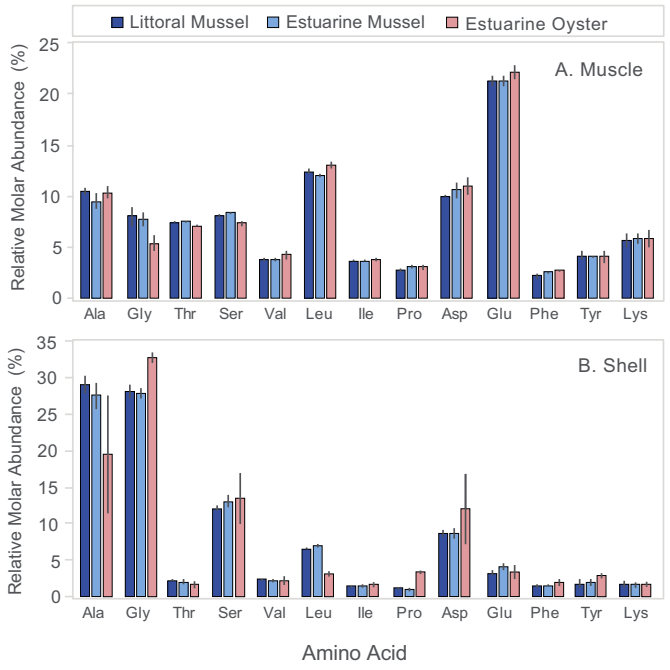

Fig. 4. Relative molar abundance of 12 amino acids measured in littoral *Mytilus californianus* (dark blue), estuarine *M. edulis* (light blue) and estuarine *O. Lurida* (light pink) in (A) soft muscle tissue and (B) shell matrix protein. Error bars indicate ±1 SD. (For interpretation of the references to colour in this figure legend, the reader is referred to the web version of this article.)

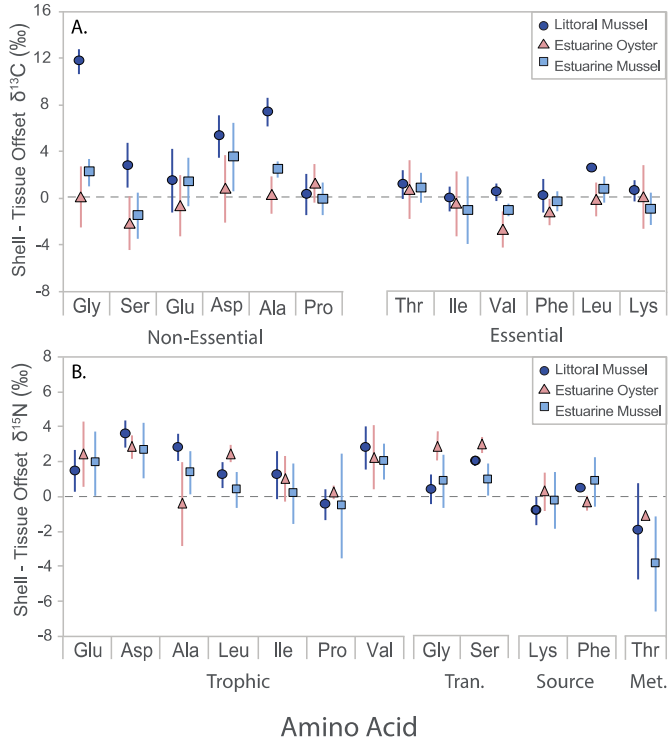

Fig. 5. Mean isotopic offset between shell and soft muscle tissue amino acid (A) $\delta^{13}C$ grouped by 'Essential' and 'Non-essential' amino acids, and (B) $\delta^{15}N$ grouped by 'Trophic', 'Transitional', 'Source' and 'Metabolic' amino acids, for three bivalve species, littoral *Mytilus californianus* (dark blue circles), estuarine *O. Lurida* (pink triangle) and estuarine *M. edulis* (light blue square). Error bars indicate ±1 SD. (For interpretation of the references to colour in this figure legend, the reader is referred to the web version of this article.)

muscle tissue, and 1.5 to 1.9 in shell. Therefore, based on our measured data we propose a new mollusk-specific formulation ($TL_{CSIA\text{-}mollusk}$), which includes a new term for observed shell vs. tissue fractionation, and also uses our empirically estimated trophic discrimination factor (TDF) values specific for mollusks:

$$TL_{CSIA-mollusk} = 1 + \left[\left(\delta^{15}N_{Glu} - \delta^{15}N_{Phe} - \beta\right) / \left(TDF_{Glu-Phe} - \varepsilon_{shell}\right)\right], \quad (4)$$

A TDF (3.4‰) combined with a fractionation factor based observed CSI-AA data offsets between soft tissue and shell ($\varepsilon = 1.6‰$), returned a very narrow range of TL values ($TL = 2.0 \pm 0.2$) across both tissue types for all three species in both environments.

4. Discussion

4.1. Tissue offsets in bulk isotopes and AA composition

Shell matrix protein versus muscle tissue offsets were remarkably consistent irrespective of season (Table 3), suggesting they are a function of biochemical composition between the tissue types, and not shifts in diet, which might influence isotopic composition of shell matrix protein and muscle tissue differently due to variability in time averaging. Bulk isotope enrichment in the biomineral fraction has previously been detected in mussel (Versteegh et al., 2011) and oyster (Ellis et al., 2014) shell. However, other studies investigating organics in bivalve shell, mostly clam species, have shown either the *opposite* or no difference in bulk isotope offsets (O'Donnell et al., 2003; Watanabe et al., 2009; Whitney et al., 2019; Graniero et al., 2021). Therefore, while data are consistent within this study, $\delta^{13}C_{bulk}$ and $\delta^{15}N_{bulk}$ offsets could be species or genera specific. And such differences could in part also be related to shell mineralogy (calcite vs. aragonite) or shell microstructure (nacreous, prismatic or homogenous). Specifically, the composition of structural proteins and other organics in whole shell may vary according to minerology of different species, which can have distinct isotope ratios (Gillikin et al., 2017). However, the generally consistent offsets between tissue types across all species (Fig. 4), in particular for CSI-AA data (Fig. 5), clearly indicates that such variation would not impact the main goals or conclusions of our paper.

In contrast to bulk isotopes, our molar AA abundance data between muscle tissue and shell matrix protein matched AA profiles typical of most muscle tissues (McMahon et al., 2010; McMahon et al., 2015; Whitney et al., 2019) and structural proteins (Hare et al., 1991; McMahon et al., 2018) (Fig. 4). However, the variation observed in several AAs in shell mol% distributions between genera is likely related to the unique compositions typical of structural proteins. It is well known that organic matrix composition varies based on shell mineralogy and microstructure (Marin and Luquet, 2004; Kobayashi and Samata, 2006). As noted above, mollusks can mineralize calcium carbonate as calcite (the more stable form), as well as aragonite (less stable form). While oysters primarily build their shells as prismatic and foliated calcite, mussels mineralize two discrete layers of calcite and aragonite, an outer prismatic calcite layer and inner nacreous aragonite layer. These differences in shell mineralogy are also associated with species-specific proteins, as reflected in the different AA molar abundances (Agbaje et al., 2018). Ala and Gly are the most abundant AAs in nacreous aragonite and Gly the most abundant AA in prismatic calcite (Kobayashi and Samata, 2006), which is consistent with our findings in mussel and oyster shells. Overall, the more variable and highly specific AA composition of shell, compared to the generally similar composition of soft tissues, may in part account for differences in bulk stable isotope offsets noted above. These observations also suggest that mol% weighted AA isotope proxies (e.g., THAA and $\delta^{13}C_{baseline}$, discussed below) may give more representative values when comparing between tissue types or across different species.

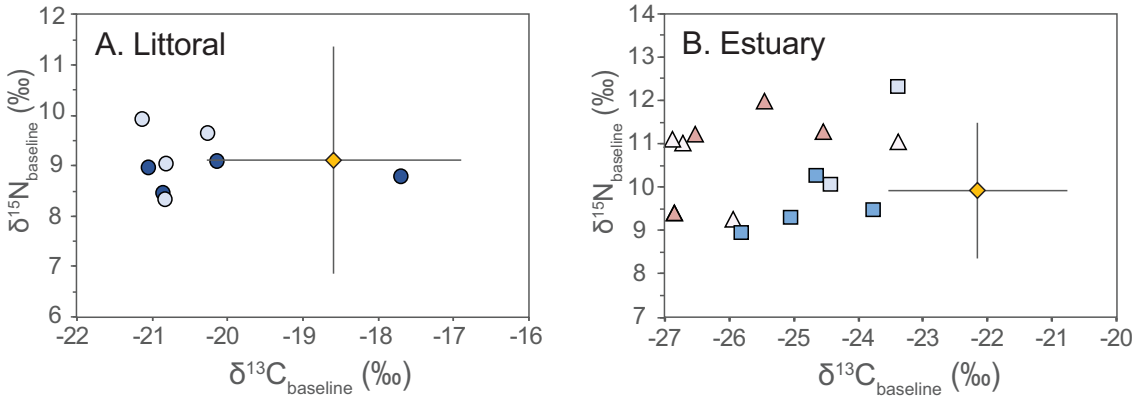

Fig. 6. Baseline production values estimated from mol% adjusted $\delta^{13}C$ essential amino acids and $\delta^{15}N$ phenylalanine values for (A) Littoral *Mytilus californianus* (circles) and (B) Estuarine *O. Lurida* (triangles) and *M. edulis* (square) in muscle soft tissue (dark shade) and shell matrix protein (light shade). Yellow diamonds indicate mean bulk $\delta^{13}C$ and $\delta^{15}N$ and standard error bars for each ecosystem's seawater POM (Nitex and GFF combined). See methods for baseline isotope values calculations. (For interpretation of the references to colour in this figure legend, the reader is referred to the web version of this article.)

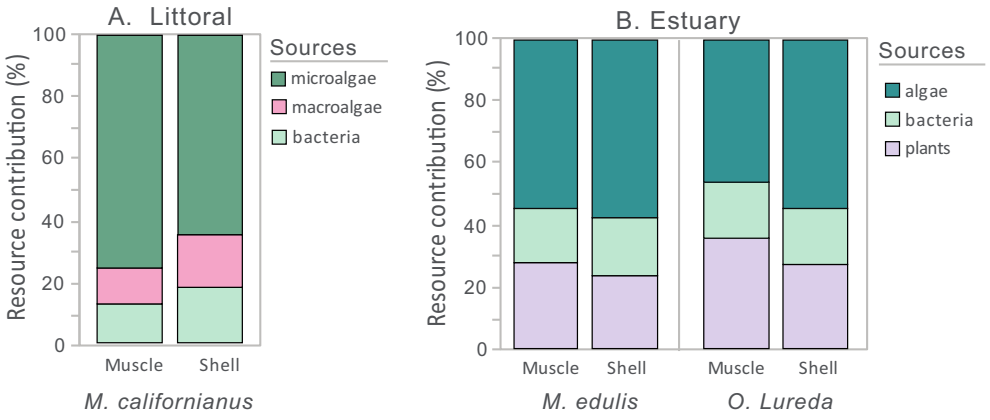

Fig. 7. Relative resource contribution of bivalve diet matches in soft tissue and shell. Estimations calculated using the Bayesian mixing model MixSIAR and is based on bivalve essential amino acid $\delta^{13}C$ values ($\delta^{13}C_{Val}$, $\delta^{13}C_{Leu}$, $\delta^{13}C_{Ile}$, $\delta^{13}C_{Thr}$, $\delta^{13}C_{Phe}$ and $\delta^{13}C_{Lys}$; median ± 95% credible intervals) and of 3 sources to the littoral environment (microalgae, macroalgae, bacteria; data from Larsen et al., 2013) and 3 sources to the estuarine environment (algae, bacteria and plants; data from Larsen et al. (2013) and Tipple et al., 2021). Note, these results are based on pre-determined input sources. The mixing model performs better with few sources, therefore, for the estuarine system, micro- and macro-algae were combined to represent algae, and aquatic- and terrestrial-plants were combined to represent plants (see data repository for training set).

4.2. Seasonal cycle control on isotope ratios

Seasonal biogeochemical cycles along central coastal California are primarily marked by a strong upwelling season in the Spring (Hickey, 1998). Annual to decadal oscillations such as ENSO and PDO, however, can affect the degree or intensity of seasonal events (Pennington and Chavez, 2017). Such dynamics raise the question if seasonal or ENSO related perturbations may be recorded and discernible in mollusk soft tissue or shell. The potential issue for shell to record seasonality is important to consider when using whole shell bioarchives for paleo reconstruction, because it's consequential to know if isotopic signals are primarily recording the single most productive season, or an average integration time represented by whole shells, typically a year to several years. Because the whole shell in this study were expected to integrate over 1–2 years, we did not expect to observe any evidence of seasonality in shell. Since soft tissue is thought to have isotopic turnover on the scale of months, by comparing these two tissues it should be possible to determine if specific seasonal isotope signatures likely detectable in soft tissue might also appear to dominate the far longer integration period of shell values. Our sampling plan therefore only targeted four main seasonal periods, since our goal was never to study detailed seasonality, but rather only to test if spring or summer periods skewed shell values. We also sampled seawater POM to provide a basic assessment of isotope signals in soft tissue vs. water column particles at the same location.

Our POM data gives a good annual integration of average POM isotopic composition but did not capture any seasonal variation. Specifically, our $\delta^{13}C$ and $\delta^{15}N$ POM records did not show seasonal variation at either site, likely a function of low sampling frequency coupled with the inherent lack of integration in a time-point POM sample. We collected seawater monthly at the littoral site and seasonally at the estuarine site; however, phytoplankton bloom events would likely not be captured by infrequent time-point sampling. To capture seasonal phytoplankton trends, we suggest POM sampling weekly or biweekly.

In contrast, clear seasonality was detected in both bivalve tissues. Both $\delta^{15}N_{bulk}$ and $\delta^{15}N_{baseline}$ (i.e., $\delta^{15}N_{Phe;}$ Fig. S4) were lowest in summer for both ecosystems in both muscle tissue and shell, although not always statistically significant. Along the coast, low summer $\delta^{15}N$ values are likely a function of incomplete utilization of the nitrate pool, typical of strong upwelling periods. However, it was somewhat surprising that both tissue types recorded approximately the same seasonal signal in $\delta^{15}N$, given the assumed differences in tissue turnover rates. As noted above, bivalves were collected between 55 and 60 mm, which correlate to 1 to 2 years (Coe and Fox, 1942; Harger, 1970), although growth rates can vary substantially (Goodwin et al., 2021, refs therein). We hypothesize that these relatively small shell lengths are likely why a summer seasonal signal was observed in shell, suggesting also that many of our shell samples at our specific sampling locations may have been closer to the lower end of age range estimate. It is possible bivalves sampled in this size range could be older than 2 years, however, this would make the magnitude of $\delta^{15}N$ seasonality even more surprising.

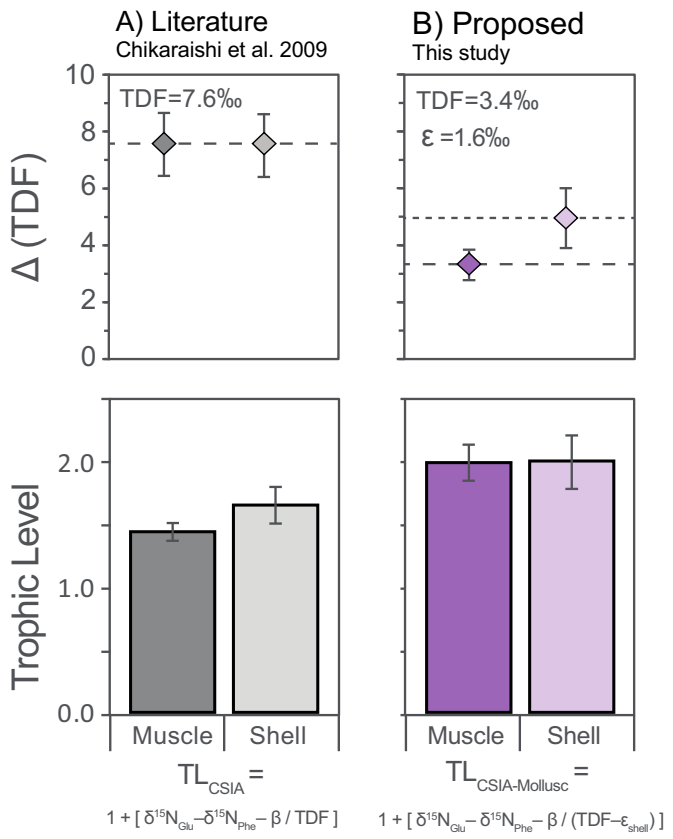

Fig. 8. Trophic level estimates calculated from the three bivalve species in this study based on amino acid $\delta^{15}N$ data from the equation proposed by Chikaraishi et al. (2009), where A) used the canonical trophic discrimination factor (TDF) Δ value = 7.6‰ in bivalve muscle (dark grey) and shell (light grey) and B) uses the newly proposed TDF value based on consistent TDFs measured in muscle (3.4‰; dark purple), and the additional hypothesized effect of 1.6‰ from isotopic routing to shell (light purple). Error bars are ±1 standard deviation. (For interpretation of the references to colour in this figure legend, the reader is referred to the web version of this article.)

Overall, this observation is consistent with the expectation that bivalves do not grow at a constant rate year-round, but rather that growth rate is known to be positively coupled with food source abundance (i.e., phytoplankton). For example, Hawkins and Bayne (1985) showed that N utilization rates and protein assimilation rates vary seasonally in *M. edulis*, with highest levels in spring/early summer (Bayne et al., 1988; Kreeger et al., 1995).

Bivalve tissue $\delta^{13}C$ values, on the other hand, did not show any clear pattern between seasonal sampling at either environment (Fig. 3, Table 3). Along the inshore CA margin, $\delta^{13}C$ signatures in mussels are a function of relative local plankton productivity and community structure and have been shown to vary with latitude (Vokhshoori et al., 2014). One prior study did observe seasonal variation in soft tissue $\delta^{13}C$ values of a clam species, *Potamocorbula amurensis,* at a southern SF bay lagoon site (Cloern, 1996), however this is a fundamentally different environment driven by tidal pumping whereas the northern SF Bay is influenced by delta inflow (Cloern, 2019), and so not likely comparable with our data. Finally, it has been shown that protein-N is more efficiently assimilated than protein-C into bivalves (Kreeger et al., 1995), which could be an additional factor underlying the apparent far lower sensitivity of the $\delta^{13}C$ record in contrast to $\delta^{15}N$. Overall, however, the lack of $\delta^{13}C$ variation suggests that at least at our sites there is not enough variation in dominant primary producer groups at times of major growth to influence bulk $\delta^{13}C$ values.

Overall, our data show that while seasonality in $\delta^{15}N$ values can be detected in both soft tissue and shell, largely driven by the productive summer upwelling season, no seasonal pattern was clearly detected in $\delta^{13}C$ values. We have hypothesized that the lower summer $\delta^{15}N$ values observed in shell is related to a combination increased summer growth with relatively small size class of our bivalves (1–2 yrs). This implies that comparison of larger shells sizes vs. soft tissue will be important in further work, since larger shell specimens are at times used for archaeological or paleo work.

4.3. Bulk and CSI-AA Ecological Isotope Proxies between tissue types

We next tested several common isotope-based ecological proxies in both soft tissue and shell protein for possible offsets in shell signatures relative to soft tissue, and to evaluate if consistent corrections could be applied to shell matrix samples for paleoecological reconstructions. These include niche width from bulk isotopes, and baseline $\delta^{13}C$, baseline $\delta^{15}N$, modeled primary producer resource contribution, and trophic level from CSI-AA.

4.3.1. Niche width bulk isotope ecological proxy

Isotopic niche width (or niche breadth) is a means to investigate the intra- and inter-individual variation of organism ecological characteristics (Newsome et al., 2007). This is a widely used measure typically based on $\delta^{13}C_{bulk}$ and $\delta^{15}N_{bulk}$ data, and is informative for understanding community composition and structure as well as resource use (e.g., Bearhop et al., 2004). *M. californianus* had a very narrow ecological niche width, in contrast to the much broader niche widths of *M. edulis* and *O. Lurida* (Fig. 2). However, between tissue types, standard ellipse area and total area were highly similar for all three species (Fig. 2), indicating that community structure and resource use is consistent within the isotope turnover times of soft tissue and shell. As noted in the previous section, Monterey Bay littoral production is dominated by two microalgal groups (e.g., diatoms and dinoflagellates; Fischer et al., 2020), as also reflected in littoral mussel soft tissue $\delta^{13}C_{EAA}$ data (Vokhshoori et al., 2014). However, mussels can additionally feed on bacteria and organic debris (Coe and Fox, 1942). While it is therefore possible for littoral mussels to feed on a broad range of suspended particulate organic sources, the narrow niche width observed suggests that at a community level, food resources are either consistently well-mixed or dominated by a few primary producer types.

In contrast, the estuarine ecosystem niche widths were very broad for $\delta^{15}N$ and $\delta^{13}C$ in both *O. Lurida* and *M. edulis*, whose niches were different from each other in carbon space (Fig. 2). In SF Bay, and delta/estuarine systems in general, it is more difficult to trace the origins of organic matter sources with bulk isotopes, because the diversity in primary production sources is much greater, coming from terrestrial, riparian, freshwater, salt marsh and marine inputs. Further, for many of these primary producer sources there is substantial isotope variability within each group, such that bulk isotope values are often broad and overlapping (Cloern et al., 2002).

There are therefore two possible hypotheses that can explain the difference in $\delta^{13}C$ niche space between *O. lurida* and *M. edulis* in the estuary. First, differences in diet between the two bivalve species. Indeed, *O. lurida* and *M. edulis* do occupy different tidal depths; *O. lurida* are low tide to subtidal dwellers (−10 to 1 m; Baker, 1995) whereas *M. edulis* occupy the mid-tide zone (2.9 to 3.2 m; Suchanek, 1978a). The lower $\delta^{13}C$ values in *O. lurida* could therefore be from a higher proportion of resuspended sediment containing degraded terrestrially derived organic matter resources (Peterson et al., 1985; Peterson and Fry, 1987). A second possibility could be characteristic organic composition differences between the species tissue; for example, the percent glycogen stores in the muscle adductor tissue. In contrast to most other animals who store energy as lipid, mollusks store it as glycogen, such that $\delta^{13}C_{bulk}$ values could reflect changes in relative glycogen content (Patterson and Carmichael, 2016). A higher glycogen content in oysters would be consistent with higher C:N ratios observed in

oyster soft tissue (3.5) vs. *M. edulis* (3.1) (data repository).

Overall, such differences in isotopic niche width between the bivalve species are important to consider when choosing a bioarchive species for historical reconstructions, or interpreting records derived from specific species. Depending on the types of environmental perturbation (e.g., drought, damming or eutrophication), one would expect a species with a narrow niche width to be more impacted, and therefore potentially a more sensitive proxy for past change. However, the most important finding for the main goals of this study was that niche widths preserved in isotopes of shell matrix protein were indistinguishable from those in muscle soft tissue in all three species. This suggests that representative niche width can be derived from well-preserved shell for historical and archaeological studies.

4.3.2. CSI-AA Baseline $\delta^{13}C$ and $\delta^{15}N$ values

Because baseline isotope reconstruction is a primary objective in palaeoecological and palaeoclimatological studies, we tested specifically whether compound-specific isotope baseline signals in soft tissue are faithfully transferred into shell, and further examined whether $\delta^{15}N_{baseline}$ and $\delta^{13}C_{baseline}$ from POM matched those integrated into both tissue types (Fig. 6). $\delta^{15}N_{baseline}$ and $\delta^{13}C_{baseline}$ from CSI-AA are integrated isotope proxies for inorganic nitrogen source (typically $\delta^{15}N_{NO3}$) and the $\delta^{13}C$ value of local primary production, respectively.

The observation that $\delta^{13}C_{baseline}$ and $\delta^{15}N_{baseline}$ from CSI-AA of shell protein overlapped with soft tissue values in both ecosystems indicates that EAAs are in fact transferred from adductor muscle to shell protein unchanged. Therefore, we conclude that no calibration or correction is required for CSI-AA baseline isotope signals in the biomineral fraction. These findings validate the use of shell samples as bioarchives which can accurately record information of past changes in sources and cycling of C and N to coastal ecosystems, as long as the shell matrix protein is well-preserved. Moreover, the isotopic offset in $\delta^{13}C_{bulk}$ niche space between *O. lurida* and *M. edulis* is not reflected at all in $\delta^{13}C_{Baseline}$ records, as might be expected. While this study cannot pinpoint the exact biological mechanism, the fact that the $\delta^{13}C_{EAA}$ match closely between the two estuarine bivalve species might suggest that observed differences in $\delta^{13}C_{bulk}$ might be a function of resynthesis of the non-essential amino acids and/or other major biomolecules.

Finally, in order to examine the relationship between baseline isotope signals incorporated into bivalves and local total particles (the overall source of bivalve food), we also compared monthly seawater POM bulk isotopic composition with bivalve baseline isotope values in both tissues (Fig. 6). We hypothesized that our $\delta^{13}C_{baseline}$ and $\delta^{15}N_{baseline}$ in bivalve tissue would directly correspond with sampled values of local seawater POM at each site. The similarity in $\delta^{15}N_{baseline}$ values observed between POM and both tissue types supports this hypothesis for both environments, while the persistent mismatch observed in $\delta^{13}C_{baseline}$ values with $\delta^{13}C$ of POM suggest selective sorting of food particles. Such sorting is well known in filter-feeders and could be linked to particular particle diameter (Defossez and Hawkins, 1997), to higher organic content (Newell and Jordan, 1983; Prins et al., 1991) or to chemical deterrence produced by the primary producer to avoid predation (Levinton et al., 2002). The specific observed $\delta^{13}C_{baseline}$ offsets from POM (Fig. 6) therefore is likely linked to the specific mixture of primary producer sources of our POM samples in each system and how much detritus is present, together representing relative nutritional value.

In the littoral ecosystem, suspended POM is predominantly a mixture of phytoplankton, macroalgae (kelp), bacteria and detrital material. $\delta^{13}C$ of kelp can vary widely along the central CA coast (−24 to −15‰; Foley and Koch, 2010), as do phytoplankton (−28 to −12‰, Rau et al., 2001), however average $\delta^{13}C$ of kelp are consistently enriched in ^{13}C relative to phytoplankton (Duggins et al., 1989). In addition, seaweeds contain chemical compounds that deter filter-feeders (polyphenolics). Macrophytes like kelp, common in the intertidal environment, also have substantially elevated C:N ratios, which in addition to high phenolic content likely decreases food value relative to single-celled algae (Levinton et al., 2002). While bivalves are known to filter-feed and ingest aged kelp where polyphenolics concentrations are significantly reduced, if available, bivalves will preferentially select phytoplankton to ingest (Levinton et al., 2002).

In the estuarine ecosystem the much larger and far more variable mismatch between $\delta^{13}C_{baseline}$ and POM suggests a far wider variety of non-utilized ^{13}C-enriched sources. This is consistent with the much greater diversity of OM sources in the estuarine environment; however, it is also more difficult to pinpoint specific sources leading to this offset. Freshwater POM is more negative (−28 ± 1.9‰) than estuarine-marine POM (−24 ± 2.2‰) (Cloern et al., 2002), and since northern SF Bay is highly influenced by freshwater inflow from the Sacramento-San Joaquin River Delta system, bivalves in this complex system are likely dynamically receiving organic matter sources for both inputs. Moreover, bivalves will adjust the particle diameter they filter-feed with changes in tides as a function of optimal organic content (Stenton-Dozey and Brown, 1992). The wide range of $\delta^{13}C_{baseline}$ (5‰) and wide niche breadth (Fig. 2) in both estuarine bivalve species therefore suggests that individuals utilize a combination of sources.

Finally, the specific CSI-AA $\delta^{13}C_{baseline}$ equation used will also have an impact on these results. Several $\delta^{13}C_{baseline}$ equations have been proposed from lab cultured phytoplankton (Vokhshoori et al., 2014), as well as for sinking (surface exported) POM in the Monterey Bay (Shen et al., 2021). The slope we derived from our $\delta^{13}C_{AA}$ POM data (Fig. S5, S6) was very similar to that reported by Shen et al. (2021). For this reason, we use Shen et al. (2021) equation to reconstruct $\delta^{13}C$ baseline values. However, where Shen et al. (2021) did not adjust for mol% (Fig. S7), our $\delta^{13}C_{EAA}$ values were mol% adjusted since soft tissue and shell protein have such different AA molar abundance distribution (Fig. 4). Overall, because there is a persistent mismatch between recorded baseline $\delta^{13}C$ signals from bivalve tissues and sampled POM, as noted above likely due to bivalves selective sorting of particles with different source $\delta^{13}C$ values (Ward and Shumway, 2004), it is not possible here to determine which equation is more correct for this application.

4.3.3. CSI-AA resource contribution

Resource contribution to bivalve diet was tested between soft tissue and shell matrix protein using a Bayesian mixing model, to determine if the biomineral fractions can be used to reconstruct relative algal and other primary production sources with application for reconstructing primary producer community structure through time. This potential has been demonstrated in deep-sea corals (McMahon et al., 2015, 2018), mussel soft tissue from both the surface (Vokhshoori et al., 2014) and deep-sea chemosynthetic environments (Vokhshoori et al., 2021), however to our knowledge the approach has never been tested in any shell matrix. The analysis depends on a “training set” of representative primary producers for a given environment having diagnostic $\delta^{13}C_{EAA}$ signatures. Larsen et al. (2009, 2013) showed that biosynthesis EAA biosynthesis carries unique “fingerprints,” and since animals cannot synthesize their own EAAs, $\delta^{13}C_{EAA}$ values pass from source to consumer without alteration. Endmembers sources used for our mixing models were specific to each sampling location and are based on the dominant primary producers in each ecosystem. For a complex system such as an estuary, there are many primary producer sources, therefore we combined primary producer groups based on broad phylogenetic associations, e.g., aquatic and terrestrial plants are in one group called ‘plants’ and micro- and macro- algae and in one group called ‘algae’.

For the littoral environment (Larsen et al., 2013 training set), our analysis predicted identical sources, within error, for both shell and soft tissue (Fig. 7). This confirms that MixSIAR is consistent with expectations from EAA CSI-AA results above. The specific sources predicted (80% of *M. californianus* diet was microalgae, followed by about 10% each from macroalgae and bacteria), a proportion which is also consistent with prior non-Bayesian resource partition results from

M. californianus soft tissue (Vokhshoori et al., 2014).

In the estuarine environment (Larsen et al., 2013 and Tipple et al., 2021 training sets), MixSIAR again indicated identical results within error in shell and muscle tissue, further confirming the application of the validity of the $\delta^{13}C_{AA}$ approach for reconstructions using both oyster and mussel shell. The specific resource partitioning showed that *M. edulis* and *O. Lurida* to be feeding the same ratio of resources (Fig. 7; 60% algae, 20% bacteria and 25% plants). The mixing model output between the two environments is consistent with the $\delta^{13}C_{bulk}$ data discussed above that bivalve diets between estuarine and littoral environments are very different. At the same time, this result highlights the potential of $\delta^{13}C_{AA}$ MixSIAR approach to bypass the limitations of $\delta^{13}C_{bulk}$ in systems with complex organic sources and indicate specific mixtures of primary production sources important in different systems.

4.3.4. Trophic level CSI-AA ecological proxy

The final ecological proxy tested was CSI-AA trophic level (TL_{CSIA}). Accurate quantification of trophic level values is key for reconstructing past ecosystems, as it can help shed light on trophic chain length of past food webs and associated nutrient abundance (Chavez et al., 2003), as well as the underpinnings of $\delta^{15}N_{bulk}$ values. For archives that primarily record POM (e.g., sediments, deep-sea corals and filter-feeders) TL_{CSIA} is typically interpreted in terms of the relative trophic structure of the plankton community, which in turn relates to relative nutrient abundance as well as climate-driven community changes (Shen et al., 2021).

However, other structural tissues as shown in deep-sea gorgonian corals has demonstrated that tissue-specific calibrations are required, due to apparent isotope routing between soft tissue and structural protein (McMahon et al., 2018; Shen et al., 2021). Therefore, a main goal was to test if similar corrections are needed in bivalve shell. Moreover, past work with bivalves suggests that the canonical TL_{CSIA} equation (with standard TDF values) does not return reasonable trophic level values for mollusks (Vokhshoori and McCarthy, 2014; Choi et al., 2018; Ek et al., 2018). Therefore, we hypothesized that existing TDF values are not appropriate for mollusk soft tissue, and that additional corrections may be required to obtain accurate TL_{CSIA} from shell.

Our results strongly bear out both of these hypotheses (Fig. 8). First, using the "canonical" CSI-AA trophic level equation proposed by Chikaraishi et al. (2009), our soft tissue results are consistent with those published previously (Vokhshoori and McCarthy, 2014), showing that the common TDF of 7.6‰ (Chikaraishi et al., 2009) is far too high for filter-feeding mollusks (i.e., resulting in too low TL_{CSIA} values). The 7.6‰ value represents the average isotope enrichment per trophic level (TDF) between $\delta^{15}N_{Glu}$ and $\delta^{15}N_{Phe}$, originally derived from controlled feeding studies of grazing zooplankton feeding on phytoplankton (McClelland and Montoya, 2002), and later confirmed by a wider range of marine grazers and consumers (Chikaraishi et al., 2007). However, none of this original work included filter-feeders, and subsequent work has shown that TDF values in fact can be highly variable between different organisms, based on both diet and specific N metabolism pathways (McMahon and McCarthy, 2016). While knowing the TL of most consumers *a-priori* is often difficult, for filter-feeding mollusks it is simplified by their predominantly algal diet, and so can be assumed to be very close to TL = 2.

Based on this assumption we use our CSI-AA data to define a new empirical TDF value for filter-feeding mollusks. Here, average $TDF_{glu\text{-}phe}$ ($\Delta^{15}N_{Glu} - \Delta^{15}N_{Phe}$) was 3.4‰, substantially below the canonical 7.6‰, and also below a revised more widely applicable $TDF_{glu\text{-}phe}$ value recently proposed by McMahon and McCarthy (2016): 6.6‰. We hypothesize the reason for the different TDF values is likely linked to specifics of mollusk N pools and turnover. $TDF_{glu\text{-}phe}$ values have generally been found to be linked to diet composition, N excretion pathway, and number of trophic steps (McMahon and McCarthy, 2016; McMahon et al., 2015; Germain et al., 2013), however different metabolic pools of protein can also be important (Chikaraishi et al., 2007). Specifically, several gastropod species have previously been shown to have "compressed" TDFs (Choi et al., 2018), which the authors hypothesized were tied to abundant N-rich protein mucus, and specifically to the high metabolic N flux required to maintain this and other high-protein structural components (i.e., proteinaceous mucus, byssal threads, squid ink, etc.). Following on this work, while empirically derived, the TDF values we propose here are not unreasonable. Further, we note that while TDF values reported in gastropods vary between species, TDF values in filter-feeding bivalves studied here are consistent (Fig. 8), irrespective of if they produce byssal threads (mussels) or not (oysters). While feeding experiments would be required to definitively verify our proposed TDF values, it seems clear that the canonical 7.6‰ TDF is far too high for filter feeding mollusks, while our proposed TDF value does yield expected TL values across environments.

Further, our shell CSI-AA data also indicates that an additional correction is required to account for tissue to shell isotope routing, consistent with past results from structural protein in deep-sea corals (McMahon et al., 2018). Specifically, as noted above the $\delta^{15}N_{Glu}$ values in shell were consistently 1.6 ± 1.1‰ higher in shell, while there was no significant difference observed in source AA (either $\delta^{15}N_{Lys}$ or $\delta^{15}N_{Phe}$) values between tissue types (Fig. 5). While we observed an *enrichment* across all our samples, it is interesting to note that is opposite compared to analogous deep-sea gorgonian coral data, which showed a 3.5‰ *depletion* in ^{15}N in structural protein compared to the metabolically active polyp tissue (McMahon et al., 2018.)

Fig. 8 synthesizes both the TDF and routing corrections required, illustrating the need for new bivalve specific CSI-AA parameters, and the impact of using traditional literature values vs. our newly proposed constants on TL_{CSIA} estimates. Using only the "literature" TDF value (7.6‰), and no routing correction, both tissue types greatly underestimated expected TL for a primary consumer, (1.4 and 1.7 muscle tissue and shell, respectively; Fig. 8), again consistent with prior data (Vokhshoori and McCarthy, 2014). While TL estimates in shell approach reasonable values (1.7 ± 0.1), this is essentially an artifact of the isotopic routing enrichment in $\delta^{15}N_{Glu}$ values demonstrated above.

Therefore, we propose a new TL_{CSIA} equations specific for soft tissue and shell protein in marine bivalves (Fig. 8), incorporating our new empirically derived TDF value of 3.4‰, with an additional fractionation factor (ε) for shell $\delta^{15}N_{Glu}$ of 1.6‰. Using the proposed new relationships returns trophic level values of 2.0 ± 0.1 in soft muscle tissue, and 2.0 in ±0.2 in shell protein. What is most important here is not the value of 2.0, since this is in some sense fixed by our assumptions, but rather the very low *variation* in TL values calculated using the same constants across both multiple species and environments. This similarity also suggests that in fact the same compressed and uniform TDF values reflect bivalve filter-feeders generally, despite differences in bulk isotope values and in food resources indicated by MixSIAR modeling.

5. Conclusions

We investigated the fidelity of bivalve shells as bioarchives for paleoecological reconstruction, comparing a suite of bulk and CSI-AA ecological isotope proxies between the well-characterized, soft muscle tissue and shell matrix protein in three bivalve species from two coastal ecosystems. We found that while shell matrix protein $\delta^{13}C_{bulk}$ and $\delta^{15}N_{bulk}$ values were consistently higher than muscle soft tissue in all three species, the trophic niche widths calculated from bulk isotope data was indistinguishable. Comparing between relatively rapid turnover of soft tissue isotope values with longer integration time of whole shells, we found no evidence for specific seasonal production biasing preserved shell isotope values. For CSI-AA derived ecological proxies, we found $\delta^{13}C_{baseline}$, $\delta^{15}N_{baseline}$ and estimation of resource contribution using MixSIAR in shell match very closely to those derived from soft tissue. However, using canonical TL_{CSIA} equations and constants, we found trophic level to be substantially underestimated in both tissue types. Based on our new data set, we therefore propose a new empirical TDF value (3.4‰) for filter-feeding mollusks, and additional ε value (1.6‰)

required for correction of TL_{CSIA} data from shell, due to isotope. Importantly, the narrow range of variation observed TL_{CSIA} values using our new relationships across species and estuarine/ littoral environments suggests these average values are accurate and widely applicable across suspension-feeding gastropods. Finally, we note that the new mollusk-specific TDF values indicated by our results is substantially below TDF ranges observed for other ammonia excreting, marine primary consumers. We therefore suggest that direct bivalve feeding experiments should be done to further explore TDF values in filter-feeding mollusks.

Overall, these results highlight the importance of conducting isotope calibration studies on any proposed new bioarchive. Because the isotopic offsets in structural protein clearly vary between organisms, we suggest that the correction factors for bioarchive structural protein are likely to be specific to organism type. This study now enables the use of well-preserved bivalve shell for archaeological and geological studies, in particular using CSI-AA data. Bivalve shell represents one of the most promising bioarchives for understanding ocean change in coastal regions, since sessile filter-feeders record biogeochemical cycling at localized nearshore environments. Coastal upwelling ecosystems are particularly physically and biologically dynamic (Chavez and Messie, 2009), and responses to climatic perturbations can be challenging to study using more tradition archives (e.g, sediments, deep sea corals). Therefore, the new data here can be used to develop bivalve shells as bioarchives, opening up entirely new suite of tracers to directly connect food web responses to physical oceanographic changes in the historical and geologic past.

Declaration of Competing Interest

The authors declare that they have no known completing financial interests or personal relationships.

Acknowledgements

We appreciate Chela Zabin from the Smithsonian Environmental Research Center for permission to collect bivalves from San Francisco Bay survey sites. We thank UC Santa Cruz's Stable Isotope Lab staff, Stephanie Christensen, Dyke Andresen and Colin Carney for assistance in bulk and amino acid isotope analysis. And we are grateful to Nancy Prouty for feedback on an earlier version of this manuscript. This work was funded by the University of California, Santa Cruz Future Leaders of Coastal Science Award.

Appendix A. Supplementary data

Supplementary data to this article can be found online at https://doi.org/10.1016/j.palaeo.2022.110979.

References

Agbaje, O.B.A., Ben, S.I., Zax, D.B., Schmidt, A., Jacob, D.E., 2018. Biomacromolecules within bivalve shells: is chitin abundant? Acta Biomater. 80, 176–187.
Baker, P., 1995. Review of ecology and fishery of the Olympia oyster, Ostrea lurida with annotated bibliography. J. Shellfish Res. 14, 501–518.
Batista, F.C., Ravelo, A.C., Crusius, J., Casso, M.A., McCarthy, M.D., 2014. Compound specific amino acid $\delta^{15}N$ in marine sediments: a new approach for studies of the marine nitrogen cycle. Geochim. Cosmochim. Acta 142, 553–569.
Bayne, B.L., Hawkins, A.J.S., Navarro, E., 1988. Feeding and digestion in suspension-feeding bivalve molluscs: the relevance of physiological compensations. Am. Zool. 28, 147–159.
Bearhop, S., Adams, C.E., Waldron, S., Fuller, R.A., Macleod, H., 2004. Determining trophic niche width: a novel approach using stable isotope analysis. J. Anim. Ecol. 73, 1007–1012.
Chavez, F.P., Messie, M., 2009. A comparison of eastern boundary upwelling ecosystems. Prog. Oceanogr. 83, 80–96.
Chavez, F.P., Ryan, J., Lluch-Cota, S.E., Ñiquen, M., 2003. From anchovies to sardines and back: multidecadal change in the Pacific Ocean. Science 299, 217–221.
Chikaraishi, Y., Kashiyama, Y., Ogawa, N.O., Kitazato, H., Ohkouchi, N., 2007. Metabolic controls of nitrogen isotope composition of amino acids in marine macroalgae and gastropods: implications for aquatic food web studies. Mar. Ecol. Prog. Ser. 342, 85–90.
Chikaraishi, Y., Ogawa, N.O., Kashiyama, Y., Takano, Y., Suga, H., Tomitani, A., Miyashita, H., Kitazato, H., Ohkouchi, N., 2009. Elucidation of aquatic food-web structure based on compound-specific nitrogen isotopic composition of amino acids. Limnol. Oceanogr. Methods 7, 740–750.
Choi, B., Takizawa, Y., Chikaraishi, Y., 2018. Compression of trophic discrimination in $^{15}N/^{14}N$ within amino acids for herbivorous gastropods. Res. Org. Geochem. 34, 29–35.
Cloern, J.E., 1996. Phytoplankton bloom dynamics in coastal ecosystems: a review with some general lessons from sustained investigation of San Francisco Bay, California. Rev. Geophys. 34, 127–168.
Cloern, J.E., 2019. Patterns, pace, and processes of water quality variability in a long-studied estuary. Limnol. Oceanogr. https://doi.org/10.1002/lno.10958.
Cloern, J.E., Canuel, E.A., Harris, D., 2002. Stable carbon and nitrogen isotope composition of aquatic and terrestrial plants of the San Francisco Bay estuarine system. Limnol. Oceanogr. 47, 713–729.
Coe, W.R., Fox, D.L., 1942. Biology of the California sea-mussel (*Mytilus californianus*) – influence of temperature, food supply, sex and age in the rate of growth. J. Exp. Zool. 90 (1), 1–30.
Defossez, J.M., Hawkins, A.J.S., 1997. Selective feeding in shellfish: size-dependent rejection of large particles within pseudofaeces from Mytilus edulis, *Ruditapes philippinarum* and *Tapes decussatus*. Mar. Biol. 129, 139±147.
Duggins, D.O., Simenstad, C.A., Estes, J.A., 1989. Magnification of secondary production by kelp detritus in coastal marine ecosystems. *Science* (Washington, D.C.) 245, 170–173.
Ek, C., Holmstrand, H., Mustajärvi, L., Garbaras, A., Bariseviciute, R., Sapolaite, J., Sobek, A., Gorokhova, E., Karlson, A.M., 2018. Using compoundspecific and bulk stable isotope analysis for trophic positioning of bivalves in contaminated Baltic Sea sediments. Environ. Sci. Technol. 52, 486–4868.
Ellis, G.S., Herbert, G., Hollander, D., 2014. Reconstructing carbon sources in a dynamic estuarine ecosystem using oyster amino acid $\delta^{13}C$ values from shell and tissue. J. Shellfish Res. 33, 217–225.
Fischer, A.D., McGaraghan, A., Hayashi, K., Kudela, R.M., 2020. Return of the "age of dinoflagellates": drivers of unusual dinoflag-ellate dominance in northern Monterey Bay examined using automated imaging flow cytometry. Limnol. Oceanogr. 65, 2125–2141. https://doi.org/10.1002/lno.
Foley, M.M., Koch, P.L., 2010. Correlation between allochthonous subsidy input and isotopic variability in the giant kelp Macrocystis pyrifera in Central California, USA. Mar. Ecol. Prog. Ser. 409, 41–50.
Germain, L., Koch, P.L., Harvey, J., McCarthy, M.D., 2013. Nitrogen isotope fractionation in amino acids from harbor seals: implications for compound-specific trophic position calculations. Mar. Ecol. Prog. Ser. 482, 265–277.
Gillikin, D., Lorrain, A., Jolivet, A., Kelemen, Z., Chauvaud, L., Bouillon, S., 2017. High-resolution nitrogen stable isotope sclerochronology of bivalve shell carbonate-bound organics. *Geochem,* Cosmochim. Acta 200, 55–66.
Goodwin, D.H., Gillikin, D.P., Jorn, E.N., Fratian, M.C., Wanamaker, A.D., 2021. Comparing contemporary biogeochemical archives from Mercenaria mercenaria and Crassostrea virginica: Insights on paleoenvironmental reconstructions. Palaeogeogr. Palaeoclimatol. Palaeoecol. 562, 110110.
Gorokhova, E., Hansson, S., 1999. An experimental study on variations in stable carbon and nitrogen isotope fractionation during growth of Mysis mixta and Neomysis integer. Can. J. Fish. Aquat. Sci. 56, 2203–2210.
Graniero, L.E., Gillikin, D.P., Surge, D., Kelemen, Z., Bouillon, S., 2021. Assessing $\delta^{15}N$ values in the carbonate-bound organic matrix and periostracum of bivalve shells as environmental archives. Palaeogeogr. Palaeoclimatol. Palaeoecol. 564, 110108. https://doi.org/10.1016/j.palaeo.2020.110108.
Hare, E.P., Fogel, M.L., Stafford, T.W., Mitchell, A.D., Hoering, T.C., 1991. The isotopic composition of carbon and nitrogen in individual amino acids isolated from modern and fossil proteins. J. Archaeol. Sci. 18, 277–292.
Harger, J.R.E., 1970. Comparison among growth characteristics of two species of sea mussels, *Mytilus edulis* and *Mytilus californianus*. Veliger 13 (1), 44–56.
Hawkins, A.J.S., Bayne, B.L., 1985. Seasonal variation in the relative utilization of carbon and nitrogen by the mussel Mytilus edulis: budgets, conversion efficiencies and maintenance requirements. Mar. Ecol. Prog. Ser. 25, 181–188.
Hickey, B.M., 1998. Coastal oceanography of western North America from the tip of Baja California to Vancouver Island. In: Robinson, A.R., Brink, K.H. (Eds.), The Sea, the Global Coastal Ocean, vol. 11. John Wiley & Sons, New York, NY, pp. 345–393.
Howland, M.R., Corr, L.T., Young, S.M.M., Jones, V., Jim, S., Van Der Merwe, N.J., Mitchell, A.D., Evershed, R.P., 2003. Expression of the dietary isotope signal in the compound-specific ?13C values of pig bone lipids and amino acids. Int. J. Osteoarchaeol. 13, 54–65.
Jackson, A.L., Inger, R., Parnell, A.C., Bearhop, S., 2011. Comparing isotopic niche widths among and within communities: SIBER - stable Isotope Bayesian Ellipses in R. J. Anim. Ecol. 80 (3), 595–602.
Jacox, M.G., Fiechter, J., Moore, A.M., Edwards, C.A., 2015. ENSO and the California current coastal upwelling response. J. Geophys. Res. Oceans 120, 1691–1702. https://doi.org/10.1002/2014JC010650.
Jassby, A.D., Cloern, J.E., Powell, T.M., 1993. Organic carbon sources and sinks in San Francisco Bay—variability induced by river flow. Mar. Ecol. Prog. Ser. 95, 39–54.
Kobayashi, I., Samata, T., 2006. Bivalve shell structure and organic matrix. Mater. Sci. Eng. C 26, 692–698. https://doi.org/10.1016/j.msec.2005.09.101.
Kreeger, D.A., Hawkins, A.J.S., Bayne, B.L., Lowe, D.M., 1995. Seasonal variation in the relative utilization of dietary protein for energy and biosynthesis by the mussel *Mytilus edulis*. Mar. Ecol. Prog. Ser. 126, 177–184.

Larsen, T., Taylor, D.L., Leigh, M.B., O'Brien, D.M., 2009. Stable isotope fingerprinting: a novel method for identifying plant, fungal, or bacterial origins of amino acids. Ecology 90, 3526–3535.
Larsen, T., Ventura, M., Andersen, N., O'Brien, D.M., Piatkowski, U., McCarthy, M.D., 2013. Tracing carbon sources through aquatic and terrestrial food webs using amino acid stable isotope fingerprinting. PLoS One 8, e73441.
Levinton, J.S., Ward, J.E., Shumway, S.E., 2002. Feeding responses of the bivalves Crassostrea gigas and Mytilus trossulus to chemical composition of fresh and aged kelp detritus. Mar. Biol. 141, 367–376.
Marin, F., Luquet, G., 2004. Molluscan shell proteins. CR Palevol 3, 469–492. https://doi.org/10.1016/j.crpv.2004.07.009.
McClelland, J.W., Montoya, J.P., 2002. Trophic relationships and the nitrogen isotopic composition of amino acids in plankton. Ecology. 83, 2173–2180.
McMahon, K.W., McCarthy, M.D., 2016. Embracing variability in amino acid $\delta^{15}N$ fractionation: mechanisms, implications, and applications for trophic ecology. Ecosphere. 7 (12), 1–26.
McMahon, K.W., Fogel, M.L., Elsdon, T.S., Thorrold, S.R., 2010. Carbon isotope fractionation of amino acids in fish mus- cle reflects biosynthesis and isotopic routing from dietary protein. J. Anim. Ecol. 79, 1132–1141.
McMahon, K.W., Guilderson, T.P., Sherwood, O.A., Larsen, T., McCarthy, M.D., 2015. Millennial- scale plankton regime shifts in the subtropical North Pacific Ocean. Science 350, 1530–1533.
McMahon, K.W., Williams, B., Guilderson, T.P., Glynn, D.S., McCarthy, M.D., 2018. Calibrating amino acid $\delta^{13}C$ and $\delta^{15}N$ offsets between polyp and protein skeleton to develop proteinaceous deep-sea corals as paleoceanographic archives. Geochemica et Cosmochimica Acta 220, 261–275.
Mompean, C., Bode, A., Gier, E., McCarthy, M.D., 2016. Bulk vs. amino acid stable N isotope estimations of metabolic status and contributions of nitrogen fixation to size-fractionated zooplankton biomass in the Subtropical N Atlantic. Deep-Sea Res. I Oceanogr. Res. Pap. 114, 137–148.
Newell, R.I.E., Jordan, S.J., 1983. Preferential ingestion of organic material by the American oyster *Crassostrea virginica*. Mar. Ecol. Prog. Ser. 13, 47–53. Newsome (2007).
Newsome, S.D., Martınez del Rio, C., Bearhop, S., Phillips, D.L., 2007. A niche for isotopic ecology. Front. Ecol. Environ. 5, 429–436.
O'Donnell, T.H., Macko, S.A., Chou, J., Davis-Hartten, K.L., Wehmiller, J.F., 2003. Analysis of $\delta^{13}C$, $\delta^{15}N$, and $\delta^{34}S$ in organic matter from the biominerals of modern and fossil Mercenaria spp. Org. Geochem. 34, 165–183. https://doi.org/10.1016/S0146- 6380(02)00160-2.
Patterson, H.K., Carmichael, R.H., 2016. The effect of lipid extraction on carbon and nitrogen stable isotope ratios in oyster tissues: implications for glycogen-rich species. Rapid Commun. Mass Spectrom. 30, 2594–2600.
Pennington, J.T., Chavez, F.P., 2017. Decade-scale oceanographic fluctuation in Monterey Bay, California, 1989–2011. Deep-Sea Res. II Top. Stud. Oceanogr. 151, 4–15. https://doi.org/10.1016/j.dsr2.2017.07.005.
Peterson, B.J., Fry, B., 1987. Stable isotopes in ecosystem studies. Annu. Rev. Ecol. Syst. 18, 293–320.
Peterson, B.J., Howarth, R.W., Garritt, R.H., 1985. Multiple stable isotopes used to trace the flow of organic matter in estuarine food webs. Science 227, 1361–1363.
Prins, T.C., Smaal, A.C., Pouwer, A.J., 1991. Selective ingestion of phytoplankton by the bivalves Mytilus edulis L. and Cerastoderma edule (L.). Hydrobiol. Bull. 25, 93±100.
Rau, G.H., Chavez, F.P., Friederich, G.E., 2001. Plankton $^{13}C/^{12}C$ variations in Monterey Bay, California: evidence of non-diffusive inorganic carbon uptake by phytoplankton in an upwelling environment. Deep Sea Res. I 48, 79–94.
Shen, Y., Guilderson, T.P., Sherwood, O.A., Castro, C.G., Chavez, F.P., McCarthy, M.D., 2021. Amino acid $\delta^{13}C$ and $\delta^{15}N$ patterns from sediment trap time series and deep-sea corals: implications for biogeochemical and ecological reconstructions in paleoarchives. Geochim. Cosmochim. Acta 297, 288–307. https://doi.org/10.1016/j.gca.2020.12.012.
Silfer, J.A., Engel, M.H., Macko, S.A., Jumeau, E.J., 1991. Stable carbon isotope analysis of amino acid enantiomers by conventional isotope ratio mass spectrometry and combined gas chromatography/isotope ratio mass spectrometry. Anal. Chem. 63, 370–374.
Stenton-Dozey, J.M.E., Brown, A.C., 1992. Clearance and retention efficiency of natural suspended particles by the rockpool bivalve Venerupis corrugatus in relation to tidal availability. Mar. Ecol. Prog. Ser. 82, 175–186.
Stock, B.C., Semmens, B.X., 2016. MixSIAR GUI User Manual. https://doi.org/10.5281/zenodo.47719. https://github.com/brianstock/MixSIAR/. Version 3.1.
Suchanek, T.H., 1978. The ecology of Mytilus edulis L. in exposed rocky intertidal communities. J. Exp. Mar. Biol. Ecol. 31, 105–120.
Tipple, B.J., Christensen, S., Ianiri, H.L., McCarthy, M.D., Vokhshoori, N.L., 2021. A new molecular isotopic toolkit to examine estuarine food webs and biogeochemistry: compound specific isotope analyses of amino acids from aquatic and terrestrial plants of the Sacramento-San Joaquin Delta. PANGAEA. https://doi.org/10.1594/PANGAEA.938300.
Versteegh, E.A.A., Gillikin, D.P., Dehairs, F., 2011. Analysis of $\delta^{15}N$ values in mollusk shell organic matrix by elemental analysis/isotope ratio mass spectrometry without acidification: an evaluation and effects of long-term preservation. Rapid Commun. Mass Spectrom. 25, 675–680.
Vokhshoori, N.L., McCarthy, M.D., 2014. Compound-specific $\delta^{15}N$ amino acid measurements in littoral mussels in the California upwelling ecosystem: a new approach to generating baseline $\delta^{15}N$ isoscapes for coastal ecosystems. PLoS One 9, e98087.
Vokhshoori, N.L., Larsen, T., McCarthy, M.D., 2014. Reconstructing $\delta^{13}C$ isoscapes of phytoplankton production in a coastal upwelling system with amino acid isotope values of littoral mussels. Mar. Ecol. Prog. Ser. 504, 59–72.
Vokhshoori, N.L., McCarthy, M.D., Close, H.G., Demopoulos, A.W.J., Prouty, N.G., 2021. New geochemical tools for investigating resource and energy functions at deep-sea cold seeps using amino acid $\delta^{15}N$ in chemosymbiotic mussels (Bathymodiolus childressi). Geobiology 00, 1–17. https://doi.org/10.1111/gbi.12458.
Ward, J.E., Shumway, S.E., 2004. Separating the grain from the chaff: particle selection in suspension and deposit feeding bivalves. J. Exp. Mar. Biol. Ecol. 300, 83–130.
Watanabe, S., Kodama, M., Fukuda, M., 2009. Nitrogen stable isotope ratio in the manila clam, Ruditapes philippinarum, reflects eutrophication levels in tidal flats. Mar. Pollut. Bull. 58, 1447–1453.
Whitney, N.M., Johnson, B.J., Dostie, P.T., Luzier, K., Wanamaker, A.D., 2019. Paired bulk organic and individual amino acid $\delta^{15}N$ analyses of bivalve shell periostracum: a paleoceanographic proxy for water source variability and nitrogen cyclin processes. Geochim. Cosmochim. Acta 254, 67–85. https://doi.org/10.1016/j.gca.2019.03.019.
Wolf, N., Newsome, S.D., Peters, J., Fogel, M.L., 2015. Variability in the routing of dietary proteins and lipids to consumer tissues influences tissue specific discrimination. Rapid Commun. Mass Spectrom. 29, 1448–1456.